Terr. Atmos. Ocean. Sci., Vol. 27, No. 6, 769-789, December 2016 doi: 10.3319/TAO.2016.09.12.01

REVIEW

Studies on Aftershocks in Taiwan: A Review

Jeen-Hwa Wang[1, *], Kou-Cheng Chen[1], Peih-Lin Leu[2], and Chien-Hsin Chang[2]

[1] *Institute of Earth Sciences, Academia Sinica, Taipei City, Taiwan, R.O.C.*
[2] *Seismological Center, Central Weather Bureau, Taipei City, Taiwan, R.O.C.*

Received 30 December 2015, revised 9 September 2016, accepted 12 September 2016

ABSTRACT

We reviewed studies on aftershocks in Taiwan for the following topics: the spatial-temporal distributions and focal-plane solutions of aftershocks fromof thirty larger earthquakes with magnitudes > 5; the correlations between the mainshock and the largest aftershock based on dependence of the differences in magnitudes (ΔM), occurrence times (ΔT), epicenters (ΔH), and focal depths (ΔD) upon the mainshock magnitude, M_m; magnitude-dependence of p-value of Omori's law of aftershocks; the correlation between the b-value of the Gutenberg-Richter's frequency-magnitude law and the p-value; application of the epidemic-type aftershock sequences (ETAS) model to describe the aftershock sequence; the mechanisms of triggering aftershocks; and dynamic modeling of aftershocks. The main results are: (1) The spatial distribution of aftershocks for some earthquakes is consistent with the recognized fault; (2) Unlike Båth's law, ΔM slightly increases with M_m; (3) ΔT does not correlate with M_m; (4) ΔD does not correlate with M_m; (5) ΔT somewhat increases with ΔD; (6) The p-value slightly increases with M_m; (7) There is a negative correlation between the b- and p-values. (8) There was seismic quiescence over a broader region of Taiwan before the 1999 Chi-Chi earthquake; (9) Both the static and dynamic stress changes trigger aftershocks; and (10) Dynamic modeling shows that a decrease in elastic modulus is a significant factor in triggering aftershocks.

Key words: Mainshock, Aftershock, Omori law, Correlation, ETAS model, Aftershock triggering, Dynamical modeling

Citation: Wang, J. H., K. C. Chen, P. L. Leu, and C. H. Chang, 2016: Studies on aftershocks in Taiwan: A review. Terr. Atmos. Ocean. Sci., 27, 769-789, doi: 10.3319/TAO.2016.09.12.01

1. INTRODUCTION

An aftershock is a smaller event that occurs after a previous large earthquake, i.e., the mainshock, in the source area. Except for swarms, most moderate and large earthquakes are often followed by aftershocks. Figure 1 shows an example of the aftershock spatial distribution occurring within about three months after the 1999 M_s7.6 Chi-Chi, Taiwan, earthquake (Ma et al. 1999; Shin and Teng 2001; Wang et al. 2005). Figure 2 displays the temporal variations in earthquake magnitude (Fig. 2a) and the number of events (Fig. 2b) for aftershocks shown in Fig. 1. Clearly, the earthquake magnitudes and frequency of events both decrease with time. Omori (1894a, b) first observed the decay in the number of aftershocks and proposed a power-law function to describe the variation in the number of aftershocks, n(t), with time, t, in the following form:

$$n(t) = k/(t + \tau) \quad (1)$$

where k and τ are two constants. This power law with a scaling exponent of 1 is called the Omori's law which is the first scaling law in both seismology and earth sciences. From experimental results, Utsu (1957) observed that the number of aftershocks decays with Omori's power law in the earlier stage but exponentially in the latter stage. Utsu (1961) modified the Omori's law to be:

$$n(t) = k/(t + \tau)^p \quad (2)$$

where p is the scaling exponent of the power-law function to modify the decay rate and typically falls in the range 0.3 - 2.0

* *Corresponding author*
E-mail: jhwang@earth.sinica.edu.tw

and often close to 1. The solid line in Fig. 2b exhibits the inferred modified Omori's law with k = 10000.0, τ = 0.8 day, and p = 1.02. Since some larger aftershocks can also generate their own aftershocks, the aftershock sequences, especially for large mainshocks, are usually very complicated, as shown in Fig. 2b. Hence, other functions have been also applied to describe aftershock sequences (cf. Utsu et al. 1995). Based on the multifractal stress activation (MSA) model which is based on thermally activated rupture and long memory stress relaxation, Ouillon and Sornette (2005) found a linear increase in the p-value with the mainshock magnitude, M_m.

Of course, the definition of an aftershock unavoidably contains a degree of arbitrariness because of implied and imprecise temporal and spatial limits. Hence, several authors (e.g., Gardner and Knopoff 1974; Molchan and Dmitrieva 1992) have proposed alternative algorithms for the selection of aftershocks.

Therefore, for both academic interests and practical needs, it is significant to explore the physical aftershock triggering processes, the transition from a mainshock to its aftershocks, and the transition from aftershock activity to background seismicity and to understand larger aftershocks because they can also cause damage (cf. Reasenberg and Jones 1989). It is difficult to predict an earthquake, but it might be possible to forecast larger-sized aftershocks after a mainshock. For academic interests and practical needs, it is necessary to study the temporal-spatial distribution of aftershocks for an earthquake, the correlations between the mainshocks and aftershocks (especially for the largest aftershock), magnitude-dependence of the p-value, and the correlation between p- and b-values of the Gutenberg-Richter's frequency-magnitude law (Gutenberg and Richter 1944) which is denoted by the GR law hereafter. In addition, it is significant to explore statistical and physical models of aftershocks.

Although Wang (2013, 2014) observed the short-term memory effect for M ≥ 6 mainshocks, others (see Lennartz et al. 2011, and cited references therein) stressed the

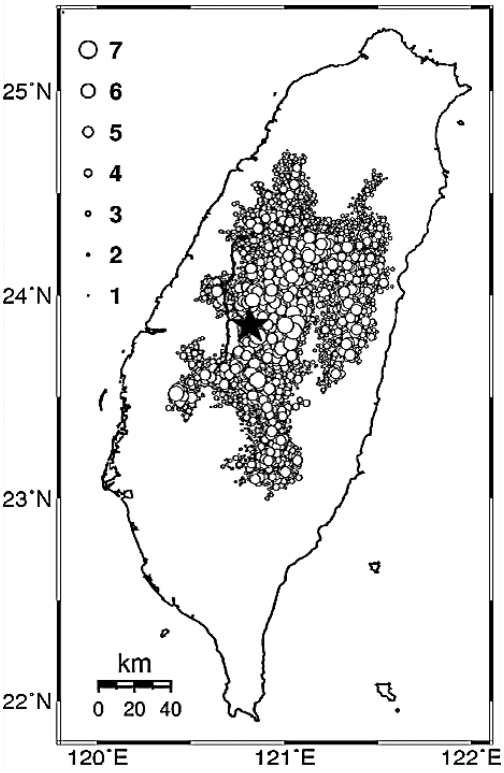

Fig. 1. The 1999 M_s7.6 Chi-Chi earthquake (shown by a solid star) and its aftershocks (displayed by open circles) occurred within 100 days after the mainshocks. The solid curve near the epicenter of mainshock denotes the Chelungpu fault.

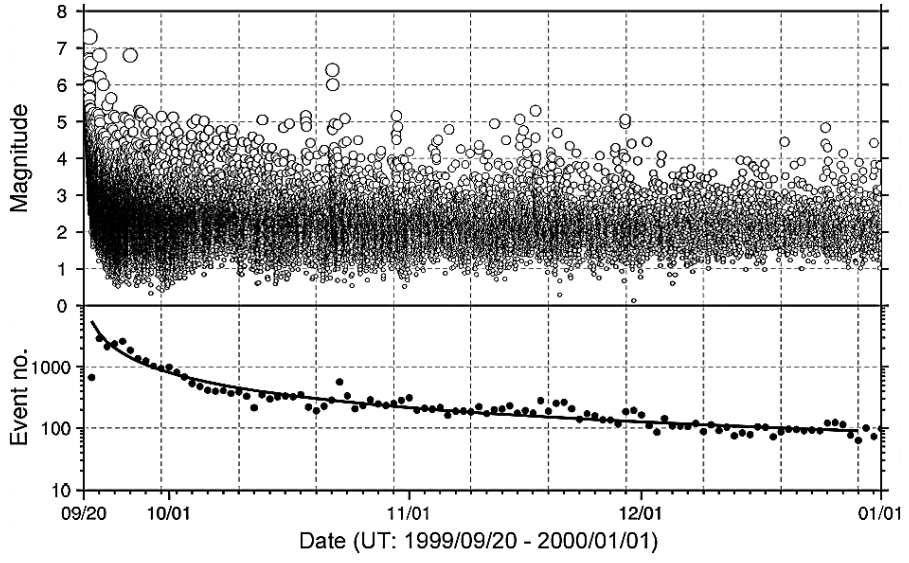

Fig. 2. The earthquake magnitude plots (a) and n(t) (b) versus t for the aftershocks shown in Fig. 1. The solid curve displays the modified Omori's law with k = 10000.0, t = 0.8 days, and p = 1.02 inferred from the data.

importance of long-term memory effect for aftershocks. The correlations between mainshock and aftershocks must be an important issue in seismology. Båth (1965) observed that the difference (ΔM) between the magnitude (M_m) of mainshock and that (M_a) of its largest aftershock is ~1.2. This is the so-called "Båth's law". Originally, ΔM is considered to be independent of M_m. But, further studies (see Chen and Wang 2012, and cited references therein) show that ΔM slightly increases with M_m and depends on the time of occurrence, seismogenic zone, heat flow, and focal depth of the mainshock. Helmstetter and Sornette (2003) assumed that the Båth's law originated from the selection procedure taken to define mainshocks and aftershocks rather than from any difference in the mechanisms controlling M_m and M_a. Using numerical simulations based on the epidemic-type aftershock sequences (ETAS) model proposed by Kagan and Knopoff (1981, 1987), Helmstetter and Sornette (2003) found that this model leads to Båth's law in a certain range of model parameters.

Utsu (1961) could not find a positive correlation between ΔT, which is the difference in occurrence times between a mainshock and its largest aftershock, and M_m for Japan's earthquakes. Båth (1984) observed that the frequency of earthquake sequence decreases with increasing ΔT for Fennoscandian earthquakes. Chen and Wang (2012) studied the dependence of the epicentral distance (ΔD) and the difference in focal depths (ΔH) between a mainshock and its largest aftershock upon M_m.

Four approaches are used to study aftershock activities. The first one is the comparison between the calculated spatial stress tensor change (including both static and dynamic triggering) caused by the mainshock and the spatial distribution of aftershocks (e.g., King et al. 1994; Kilb et al. 2000; Stein 2003; Freed 2005; Felzer and Brodsky 2006; Wang et al. 2010, 2013). The second one is statistical analysis (e.g., Kagan and Knopoff 1981; Ogata 1988; Utsu et al. 1995). The third one is aftershock modeling based on crack models (e.g., Miyatake 1985; Yamashita and Knopoff 1987; Shaw 1993; Ziv and Rubin 2003; Shcherbakov and Turcotte 2004) the self-organized criticality model (e.g., Bak and Tang 1989; Huang et al. 1998), and dynamic spring-slider models (e.g., Knopoff et al. 1982). The forth one is the application of rock fracture experiments on understanding aftershocks (e.g., Mogi 1962; Scholz 1968; Hirata 1987; Main et al. 1992; Shearer 2012).

Studies concerning the following topics are reviewed in this work: the spatial-temporal distributions of aftershocks in some Taiwan's larger earthquakes with magnitudes > 5; the correlations between a mainshock and its largest aftershock in terms of source parameters such as M_m, ΔM, ΔT, ΔD, and ΔH; magnitude-dependence of p-value; the correlation between the b- and p-value; the application of the ETAS model to describe aftershocks; the mechanisms of aftershock triggering; and aftershock dynamic modeling.

2. SEISMIC OBSERVATIONS IN TAIWAN

Taiwan (from 119 - 123°E and 21 - 26°N) is located at the juncture of the Eurasian and Philippine Sea plates (Tsai et al. 1977; Wu 1978; Lin 2002). High and heterogeneous seismicity in Taiwan makes the region one of the best natural laboratories for seismological studies. Hence, seismicity studies have been performed in Taiwan for a long time (Wang 1988, 1998, 2008; Wang and Shin 1998).

Damage reports for earthquakes that occurred before 1896 are available only from historical documents (cf. Hsu 1983). In 1897 when the Japanese occupied Taiwan, routine seismological observations were started at Taihoku (Taipei) Meteorological Observatory (TMO), which was a local office of the Central Meteorological Observatory (CMO), Japan. A history on the seismic network construction during the Japanese period can be found in Shin and Chang (2005, and cited references herein). A simple description is given below. Japan's seismologists installed the first seismometers in Taiwan, constructing 17 stations, each equipped with three-component, low-gain displacement seismometers. Old-fashioned accelerometers were also installed at some stations. All seismic records were in the analog form. The clocks at the stations were not synchronized because the technicians at the local stations individually timed the clocks. This is the main shortcoming of the network. There were remarkable errors for the arrival times, thus resulting in high uncertainty in earthquake location (Chan and Wang 1990). At the end of the Second World War, this seismic network was transferred to the Taiwan Weather Bureau (TWB), which is now the Central Weather Bureau (CWB) (see Lee 1985). An earthquake data bulletin including the phases and arrival times has been published since 1953 (four volumes annually) by the TWB and later by the CWB. The magnitude scale used in this period was Hsu's magnitude, i.e., M_H, which is comparable with the surface-wave magnitude, M_s (Wang 1992).

From 1973 - 1992, the Taiwan Telemetered Seismographic Network (TTSN) was operated by the Institute of Earth Sciences, Academia Sinica (ASIES) (see Wang 1989). This network consisted of 24 stations, each equipped with a vertical, high-gain, analog velocity seismometer. An earthquake catalogue including four volumes per year was published by the ASIES. The magnitude scale used in this period was the duration magnitude, M_D (Wang 1992).

In 1991, the Taiwan Seismic Network (TSN), operated by the CWB, was upgraded from the old CWB seismic network. Many new seismic stations were constructed. In 1992, the TTSN was merged into the TSN. At present the TSN is composed of 72 stations, each equipped with three-component, digital velocity seismometers (see Shin 1992). These seismograms record in both high- and low-gain forms. This network provides high-quality digital earthquake data. The TSN's magnitude scale is the simulated local magnitude, M_L (Shin 1995).

In addition, the Taiwan Strong Motion Instrumentation Program (TSMIP) is operated by the CWB. For details about this network, see Liu et al. (1999) and Shin and Chang (2005). This network consists of about 1000 stations, each equipped with tri-axial force-balanced accelerometers, with a full scale of ±2 g. The accelerograph used is mainly the Teledyne Geotech A900, which has a flat instrument response with a high-cut filter at 50 Hz. Some stations have recently been equipped with other types of accelerographs. The recordings are digitized with 16-bit resolution at 200 samples per second. Together with the data reported by the TSN, the recordings from this network were used to locate the events plotted in Fig. 2.

As mentioned above, the earthquake magnitudes used in various time periods are different: M_H in the TMO and TWB periods, M_D in the TTSN period, and M_L in the CWB period. Wang (1992) studied the relationships between two earthquake magnitudes. Shin (1993) inferred a formula to calculate the local magnitude, M_L, to quantity earthquakes in Taiwan from the simulated Wood-Anderson seismograms of the short-period seismograms. Shin (1993) also related M_L to other earthquake magnitudes, including M_D used in the TTSN period. In order to study the spatial-temporal distributions and modified Omori law of aftershocks, a lower-bound magnitude, M_c, is usually necessary for taking data. Since different earthquake magnitudes were used in various time periods, M_c should be different in respective time periods. Hence, the spatial-temporal distributions and modified Omori laws of aftershocks for the mainshocks that occurred in various time periods must be carefully compared.

3. STUDIES OF AFTERSHOCKS FOR INDIVIDUAL EARTHQUAKES

Historical earthquakes (e.g., Hsu 1983) are not reviewed here due to higher uncertainty in the earthquake locations. We only considered the instrumentally-recorded aftershocks studied by a researcher or group of researchers and the results formally published in research papers and/or technical reports. Based on the occurrence times of the mainshocks, seismic observations are divided into four periods, i.e., the TMO, TWB, ASIES, and CWB periods. The focal depth of an event is denoted by the symbol "H". The strike, dip and rake of the fault-plane solution for an event are denoted, respectively, by θ, ϕ, and λ. In the following, the symbol "h" is used to denote the hour. For some earthquakes, the surface-wave magnitude, M_s, and body-wave magnitude, m_b, are also given. The source parameters and geographic location for each mainshock in use are listed in Table 1. The epicenters of mainshocks in use are shown in Fig. 3. Three kinds of circles with different size denote three magnitude ranges: large size for $M \geq 7$, moderate size for $6 \leq M < 7$, and small size for $5 \leq M < 6$. The number inside each circle denotes the number of event listed in Table 1.

3.1 Earthquakes Occurred in the CMO (or TMO) Period

3.1.1 The Meishan Earthquake of 17 March 1906

An earthquake with M_H7.1 was located at (20°N, 122°E). The mainshock, aftershocks, and damages were reported in the Special Report of the CMO. Omori (1907a, b, 1908) studied several larger aftershocks.

3.1.2 The Offshore Ilan Earthquake of 2 September 1922

An earthquake with M_H7.7 was located at (24.6°N, 122.2°E). Nakamura (1922) studied its largest aftershock with M_H7.1.

3.1.3 The Hsinchu-Taichung Earthquake of 21 April 1935

An earthquake with M_H7.1 was located at (24.33°N, 120.63°E) with H = ~10 km (Kawasumi and Honma 1936). The studies about the mainshock, aftershocks and damage were also given in the following journals and reports: (1) The Supplementary Volume of Bulletin of the Earthquake Research Institute, Tokyo Imperial University in 1936; (2) Report of the Hsinchu-Taichung Earthquake in Quarterly Journal of Seismology (Vol. 9, No. 1) published by the CMO in 1935; (3) Special Report of the TMO in 1936; and (4) A report of damage by the Government of Taiwan in 1936. Yen (1985) described the earthquake and related local geology. Sheu et al. (1982) and Huang and Yeh (1992) studied the earthquake fault mechanism and slip model. Huang and Yeh (1992) measured the seismic moment and stress drop of the July 17 aftershock. Nasu (1936a) observed that most of the aftershocks, with H = ~0 km, occurred from August to December in 1935 and located to the west of the earthquake fault. Some shallow aftershocks with H < 5 km occurred very close to the earthquake fault and in the hanging wall. Nasu (1936b) reported the aftershock activity from 21 April to 31 August 1935. Lee et al. (1985) relocated the 15 relatively larger aftershocks. Since they did not show the spatial distribution of those events, we cannot further discuss their results.

3.1.4 The Chungpu, Chiayi Earthquake of 17 December 1941

An earthquake with M_H7.1 was reported by the CMO in 1942. About 1257 aftershocks occurred from 19 December 1941 to 28 February 1942 and the number of aftershocks decayed with time. Cheng et al. (1996) re-located the mainshock, whose epicenter is (23.40°N, 120.46°E) with H = 12 km, and 50 aftershocks and also determined the fault-plane solutions of some large aftershocks.

3.2 Earthquakes Occurred in the TWB Period

3.2.1 The Haulien Earthquake of 22 October 1951 (21 October, 21 h 34 m GMT)

An earthquake with M_H7.3 was located at (23.80°N, 121.70°E). Su (1985) showed that aftershocks were located almost on a plane with $\phi = 45°$ dipping to the east. Chen et al. (2008a) reported a group of M_H6+ aftershocks nearby. The M_H6.0 Chihshang earthquake occurred 34 days later and 100 km away from the mainshock. The M_H7.3 Yuli earthquake followed 3 minutes later and 5 km away from the Chihshang event. Two days later, the M_H6.0 Taitung earthquake shocked a region 40 km away from the preceding M_H6 event and completed the sequence.

3.2.2 The Offshore Hengchun Earthquake of 15 August 1959

An earthquake with M_H7.1 was located at (21.7°N, 121.3°E) with H ≈ 20 km. Lu (1960) observed that the earthquake aftershocks were located along the NW-SE direction and the number of aftershocks decayed with time.

3.2.3 The Paiho Earthquake of 18 January 1964

An earthquake with M_H6.3 was located at (23.2°N, 120.6°E) with H ≈ 18 km. Hsu and Lu (1969) observed that 236 aftershocks were located along the NW-SE direction with relative to the mainshock.

Table 1. Source parameters of mainshocks used in this study: date, epicenter, focal depth (H), earthquake magnitude (M), and geographic location.

No.	Date	Epicenter (°N, °E)	H (km)	M	Geographic Location
1	1906/03/17	(20.00°N, 122.00°E)		M_H7.1	Meishan
2	1922/09/02	(24.60°N, 122.20°E)		M_H7.7	Offshore Ilan
3	1935/04/21	(24.33°N, 120.63°E)	10	M_H7.1	Hsinchu-Taichung
4	1941/12/17	(23.40°N, 120.46°E)	12	M_H7.1	Chungpu
5	1951/10/22	(23.80°N, 121.70°E)		M_H7.3	Haulien
6	1959/08/15	(21.70°N, 121.30°E)	20	M_H7.1	Offshore Hengchun
7	1964/01/18	(23.03°N, 120.01°E)	18	M_H6.3	Paiho
8	1972/04/24	(23.50°N, 121.40°E)	20	M_D6.9	Juisui
9	1973/12/24	(24.21°N, 121.22°E)		M_D5.3	Tachien
10	1976/04/14	(23.35°N, 120.70°E)	7.7	M_D5.3	Wufeng
11	1978/07/23	(22.35°N, 121.33°E)	6.1	M_D6.8	Lanhsu
12	1983/05/10	(24.46°N, 121.51°E)	1.2	M_D5.7	Taipingshan
13	1986/05/20	(24.08°N, 121.59°E)	10.0	M_D5.9	Hualien
14	1986/11/14	(23.99°N, 121.83°E)	13.9	M_D7.2	Offshore Haulien
15	1990/12/13	(23.88°N, 121.55°E)	8.0	M_D6.7	Hualien
16	1991/03/12	(23.25°N, 120.08°E)	11.8	M_L5.7	Chiali
17	1992/04/19	(23.84°N, 121.57°E)	8.1	M_L5.6	Shilin
18	1992/04/20	(24.45°N, 120.71°E)	8.8	M_L5.2	Sanyi
19	1992/05/28	(23.13°N, 121.35°E)	13.7	M_L5.2	Chenkung
20	1992/07/07	(24.40°N, 121.73°E)	27.8	M_L5.2	Nano
21	1993/12/15	(23.21°N, 120.52°E)	12.5	M_L5.7	Tapu
22	1994/09/16	(22.43°N, 118.47°E)	13.0	M_L6.5	Taiwan Strait
23	1998/07/17	(23.50°N, 120.66°E)	2.8	M_L6.2	Ruey-Li
24	1999/09/20	(23.85°N, 120.82°E)	8.0	M_L7.3	Chi-Chi
25	1999/10/22	(23.52°N, 120.42°E)	16.6	M_L6.4	Chia-Yi
26	2003/12/10	(23.10°N, 121.34°E)	10.0	M_L6.8	Chengkung
27	2006/12/26 2006/12/26	(21.67°N, 120.56°E) (21.97°N, 120.42°E)	44.0 50.0	M_L7.1 M_L6.9	Pingtung
28	2008/03/04	(23.20°N, 120.71°E)	11.3	M_L5.2	Taoyuan
29	2010/03/04	(22.97°N, 120.71°E)	22.6	M_L6.4	Jiashan
30	2013/10/31	(23.54°N, 121.39°E)	14.6	M_L6.4	Offshore Hualien

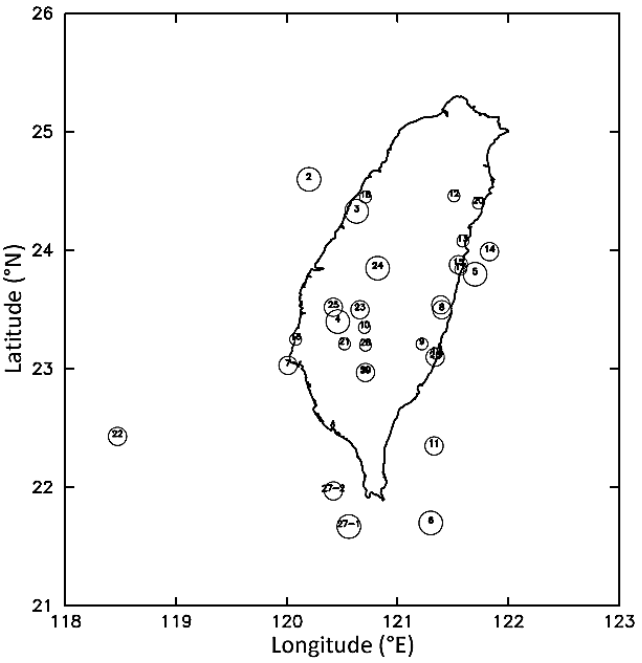

Fig. 3. The earthquake epicenters used in section 3. Three kinds of circles with different size denote three magnitude ranges: large size for $M \geq 7$, moderate size for $6 \leq M < 7$, and small size for $5 \leq M < 6$. The number inside each circle denotes the event numbers listed in Table 1.

3.3 Earthquakes Occurred in the ASIES Period

3.3.1 The Juisui Earthquake of 24 April 1972

An earthquake with M_D6.9 was located at (23.50°N, 121.40°E) with H ≈ 20 km. Lu et al. (1976) reported that the mainshock showed thrust faulting; 394 aftershocks were located almost to the north of the mainshock and the number of aftershocks decayed with time. The epicentral distribution of eleven aftershocks re-located by Chiang et al. (1986) shows NNE-SSW-striking, with southeastward increase in focal depths. Focal-plane solutions exhibit thrust faulting with the maximum stress in the NW-SE direction. Wang et al. (1992a) observed that the earthquake sequence occurred on the boundary between the Eurasian and Philippine Sea Plates.

3.3.2 The Tachien Earthquake of 24 December 1973

An earthquake with M_D5.3 was located at (24.21°N, 121.22°E). Lu (1974) observed that the fault-plane solution exhibits a left-lateral strike-slip fault with θ = N24°W and ϕ = 80°NE, and the focal depths of aftershocks range from 0 - 8 km, with the peak frequency at a depth of 5 km.

3.3.3 The Wufeng Earthquake of 14 April 1976

An earthquake with M_D5.3 was located at (23.35°N, 120.70°E) with H = 7.7 km. Yu et al. (1977) observed that most of the aftershocks were located between the Chashan thrust fault and the Tatou fault and exhibited N-S-trending. The aftershock distribution and fault-plane solutions suggest a thrust fault with θ = N5°E and ϕ = 60°W. However, the earthquake fault is not one of the two known faults.

3.3.4 The Lanhsu Earthquake of 23 July 1978

An earthquake with M_D6.8 was located at (22.35°N, 121.33°E) with H = 6.1 km. Lee and Tsai (1981) observed that some aftershocks show strike-slip faulting, yet not for others. Aftershock activity lasted, at least, for one year. Chou and Wang (1992) inferred that the mainshock consisted mainly of two sub-events, and aftershocks happened in the area which did not fail during the mainshock.

3.3.5 The Taipingshan, Ilan, Earthquake of 10 May 1983

An earthquake with M_D5.7 was located at (24.46°N, 121.51°E) with H ≈ 1.2 km. Chen and Wang (1984) observed that the mainshock was a normal fault (θ = N36°W and ϕ = 40°SW) which agrees with the trend of the aftershock zone (about 30 km long and 11 km wide). Larger foreshocks and $M_D \geq 4$ aftershocks were located mainly to the north of the mainshock.

3.3.6 The Hualien Earthquake of 20 May 1986

An earthquake with M_D5.9 was located at (24.08°N, 121.59°E) with H ≈ 10 km. Chen and Wang (1986) showed that the mainshock was a thrust fault (θ = N35°E and ϕ = 60°SE). The hypocentral distribution of the earthquake sequence displays a plane, whose extension upward to the ground surface meets a known fault, extending about 23 km in depth with ϕ = ~60°SE. Liaw et al. (1986) observed two clusters of aftershocks. In one cluster, the composite fault-plane solution shows θ = N26°E and ϕ = 80°SE. The hypocentral distribution shows a high-angle dip to the southeast. Wang et al. (1989) observed that the coda-Q was lower for aftershocks than for foreshocks, thus indicating an increase in crustal inhomogeneities after the mainshock.

3.3.7 The Offshore Haulien Earthquake of 14 November 1986

An earthquake with M_D6.1 (M_s7.8) was located at (23.99°N, 121.83°E) with H = 13.9 km. Chen and Wang (1988) observed that this earthquake was about 27 km to the ESE of the May 20 event and showed a thrust fault (θ = N33°E and ϕ = 58°SE) which is similar to that of the May 20 event. The aftershock distribution of this earthquake overlapped with that of the May 20 event, and the related fault dips to the southeast and extends to a depth of about 38 km. This is consistent with the result by Wang et al. (1992b).

3.3.8 The Hualien Earthquake of 13 December 1990

An earthquake with M_D6.7 was located at (23.88°N, 121.55°E) with H = 8 km. Wang et al. (1992b) observed that the distribution of aftershocks exhibits a plane dipping to southeast.

3.4 Earthquakes Occurred in the CWB Period

3.4.1 The Chiali Earthquake of 12 March 1991

An earthquake with M_L5.7 was located at (23.25°N, 120.08°E) with H = 11.8 km. Shin et al. (1994) reported that the earthquake shows left-lateral strike-slip faulting ($\theta = 315°$, $\phi = 60°$, and $\lambda = -5°$). The highest number of aftershocks appeared on 12 March, and the number then decayed with time. The hypocentral distribution of relocated aftershocks shows a fault plane with $\phi = 60°$ to the northeast.

Ma and Chen (1999) found that except for one event, the focal-plane solutions of numerous aftershocks exhibit an N-S-striking and N-W-dipping thrust fault.

3.4.2 Earthquakes Occurring in 1992

Shin and Chang (1992) studied the focal-plane solutions and spatial distributions of aftershock activities of four $M_L \geq 5$ earthquakes in 1992. The M_L5.6 Shilin earthquake of 19 April was located at (23.84°N, 121.57°E) with H = 8.1 km and showed a thrust fault ($\theta = 195°$, $\phi = 45°$ to the west, and $\lambda = 20°$). The M_L5.2 Sanyi earthquake of 20 April was located at (24.45°N, 120.71°E) with H = 8.8 km and showed a thrust fault ($\theta = 280°$, $\phi = 35°$ to the N, and $\lambda = -145°$). The M_L5.4 Chenkung earthquake of 28 May was located at (23.13°N, 121.35°E) with H = 13.7 km and showed a thrust fault ($\theta = 20°$, $\phi = 60°$ to the SE, and $\lambda = 40°$). The M_L5.2 Nanao earthquake of 7 July was located at (24.40°N, 121.73°E) with H = 27.8 km and showed a thrust fault ($\theta = 20°$, $\phi = 75°$ to the SW, and $\lambda = 35°$).

3.4.3 The Tapu Earthquake of 15 December 1993

An earthquake with M_L5.7 was located at (23.21°N, 120.52°E) with H = 12.5 km (Chang and Shin 1994). Kuo et al. (1994) observed that the earthquake occurred on a thrust fault ($\theta = 213°$, $\phi = 40°$, and $\lambda = 96°$) based on the aftershock distribution. From the focal-plane solution, Shin (1995) observed that the earthquake is a thrust fault ($\theta = 200°$, $\phi = 40°$, and $\lambda = 90°$) and most of the aftershocks with $M_L \geq 4$ had a faulting type similar to the mainshock. The source parameters of five larger aftershocks inferred by Shin (1995) suggested a thrust fault ($\theta = 20°$, $\phi = 48°$, and $\lambda = 84°$).

3.4.4 The Taiwan Strait Earthquake of 16 September 1994

An earthquake with M_L6.4 (m_b6.5, M_s7.3) was located at (22.43°N, 118.47°E) with H = 13 ± 3 km. Kao and Wu (1996) found that the earthquake is a high-angle normal fault ($\theta = 103°$, $\phi = 55°$, and $\lambda = -74°$) and the aftershock distribution suggests an S-dipping fault plane. They also deeply discussed the tectonic implication of the earthquake sequence. Chen et al. (1996) plotted the spatial distribution of its aftershocks with $M_L \geq 3$ occurred from 16 September 1994 to 31 May 1995 recorded by the Fujian Seismic Network. Like Kao and Wu (1996), their result also suggests an S-dipping fault plane, even though the data points are scattered. Chen et al. (1996) also inferred the modified Omori law, with $\tau = 0.96$ day and $p = 0.50$, from the aftershock sequence.

3.4.5 The Ruey-Li, Chia-Yi, Earthquake of 17 July 1998

An earthquake M_L6.2 was located at (23.50°N, 120.66°E) with H = 2.8 km. Chen et al. (1999) observed an S-E-dipping aftershock hypocenter distribution.

3.4.6 The Chi-Chi Earthquakes of 20 September 1999

An earthquake with M_L7.3 (M_s7.6) was located at (23.85°N, 120.82°E) with H = 8 km (Ma et al. 1999; Shin and Teng 2001; Wang et al. 2005). Figure 1 displays the epicenteral distribution of the mainshock and aftershocks that occurred within about 3 months after the mainshock. Figure 2 displays the temporal variations in earthquake magnitude (Fig. 2a) and n(t) (Fig. 2b) for aftershocks shown in Fig. 1. Clearly, the earthquake magnitudes and numbers of events both decrease with time. The solid line in Fig. 2b exhibits the inferred modified Omori law with $k = 10000.0$, $\tau = 0.8$ day, and $p = 1.02$.

From the plot of frequency versus magnitude for 296 aftershocks with $M_L \geq 3.4$ within the first hour after the mainshock, Chang et al. (2007) concluded that the catalog is complete when $M_L \geq 4.3$ and the b-value is about 1 for $4.3 < M_L < 6$. Most of the aftershocks occurred in a small-slip area immediately to the north of the mainshock and migrated downward from the mainshock hypocenter. Later in the hour, the aftershocks began to concentrate in the fringe area of the main rupture.

From more than 40 relocated aftershocks and their fault-plane solutions together with subsurface geology, Kao and Chen (2000) showed that the dominant seismogenic structure is a thrust fault with $\phi = 20$ to 30° away from the deformation front. A second, sub-parallel seismic zone lies about 15 km below the main thrust. These seismic zones differ from previous models, indicating that both the basal decollement and relic normal faults are aseismic.

From re-located aftershocks and their focal-plane solutions, Chen et al. (2002) observed that the hypocenters can clearly define the geometrical structure of related faults. The mainshock and two large aftershocks with $M_L = 6.8$ are all

thrust faulting on an N-S-striking fault plane dipping to the east. A group of deeper aftershocks with two moderate events (M_L = 6.3 and 6.0, respectively) exhibits a conjugate-fault system in the southern part of the source area, that is, a westward-dipping fault related to the two moderate aftershocks is conjugate to the eastward-dipping Chelungpu fault.

Chen et al. (2006) correlated the b-value to the fractal dimension (cf. Mandelbrot 1982; Wang and Lee 1996, 1997; Turcotte 1997), D, of hypocenters of aftershocks. Over 6 months after the main shock there was a positive correlation between b and D, which is in agreement with the relation D = 3b/c proposed by Aki (1981), yet opposite to those by Hirata (1989) and Wang and Lee (1996).

Based on the Z-test (Meyer 1975), Wu and Chen (2007) observed that the seismicity before and after the mainshock exhibited "seismic reversal" proposed by Shebalin and Keilis-Borok (1999). In Period I (from 1994 - 1998), normal seismicity pattern of most of the epicenters occurred in eastern Taiwan. From 1 January 1999 to 19 September 1999, the pattern indicated an abnormal stage of "seismic reversal" for the critical condition of the Chi-Chi earthquake. From 20 September 1999 to the end of 2001, seismicity marked a re-adjustment phase of crustal stress by the presence of a large number of aftershocks. From 2002 - 2005, seismicity diffused from Central Taiwan to the other areas and finally returned to eastern Taiwan.

Huang and Wang (2002, 2009) and Huang et al. (2002) measured the seismic radiation energy, E_s, and seismic moment, M_o, of twenty-two aftershocks with $5.1 \le M_L \le 6.5$. They eliminated the site effect (Huang et al. 2005) and finite frequency band width limitation effect (Wang and Huang 2007). Results are $E_s = 2.0 \times 10^{18}$ - 8.9×10^{21} g cm^2 sec^{-2} and $M_o = 1.3 \times 10^{23}$ - 1.4×10^{26} g cm^2 sec^{-2}, which give the scaled energy $E_s/M_o = 7.4 \times 10^{-6}$ - 2.6×10^{-4}. They found that E_s/M_o depends upon M_s when both E_s and M_o are evaluated from local seismograms; while E_s/M_o is independent of M_s when M_o is estimated from teleseismic data. E_s/M_o slightly depends on the focal depth, h (in km). In addition, the corner frequency, f_c, ranges from 0.15 - 1.34 and $M_o \sim f_c^{-3.65}$.

The 3-D velocity models inferred by Kim et al. (2010) showed that the mainshock occurred within a narrow low-velocity zone along the Chelungpu fault. A sudden increase in velocity and seismicity took place across the Shuilikeng fault to the east. Most aftershocks were located in areas of high V_P and high V_S. A sharp east-dipping zone extending from the surface trace of the Shuilikeng fault to a depth of ~15 km separates the low-velocity region in the west from the high-velocity region in the east. An apparent high-angle, west-dipping seismic zone lies at depths of 15 - 30 km beneath the western Central Range. Numerous aftershocks with normal faulting were located to the west of the middle segment of the Chelungpu fault.

Lee et al. (2013b) observed that the distribution of intercurrence times between aftershocks follow a non-homogeneous Poisson process. Based on the Omori time concept, which is defined as the mean inter-event time over a fixed number of aftershocks, they found that during the period 1999 after the mainshock to 2008, the seismicity rate decayed with the exception of a burst of seismicity in 1999. The distribution of Omori times during 2000 - 2008 was in good agreement with the theoretical expectation. During 1994 - 1999, the seismicity rate was relatively stable.

3.4.7 The Chia-Yi Earthquake of 22 October 1999

An earthquake with M_L6.4 was located at (23.52°N, 120.42°E) with H = 16.6 km. Chen et al. (2008b) recognized two major clusters of aftershocks with H = 10 - 16 km. One cluster with $\theta = 32°$ and $\phi = 90°$ is related to the Meishan fault along which the 1906 earthquake ruptured. The other with $\theta = 190°$ and $\phi = 64°$ to the west exhibits a west-verging reverse fault, in contrast to previous expectation of east-vergence. The focal-plane solutions of larger aftershocks together with the 3-D distribution of all events during 1990 - 2004 suggest un-recognized seismogenic zones in the area.

3.4.8 The Chengkung Earthquake of 10 December 2003

An earthquake with M_L6.8 was located at (23.10°N, 121.34°E) with H = 10.0 km. From relocated aftershocks and the focal-plane solutions of several larger aftershocks, Kuochen et al. (2007) divided the Chengkung earthquake sequences into three seismic clusters: (1) a main cluster coincided with the east-dipping background seismicity; (2) a small cluster beneath the southern end of the Chihshang fault; and (3) a cluster on the western side of the Luyeh fault.

3.4.9 The Pingtung Offshore Earthquake Doublets of 26 December 2006

Two earthquakes with M_L7.1 and M_L6.9, respectively, occurred offshore Pingtung, southwestern Taiwan. The first one occurred at 1226 UTC and was located at (21.67°N, 120.56°E) with H = 44 km. Eight minutes later, the second one happened at (21.97°N, 120.42°E) with H = 50 km. The latter was about 36 km to the north-northeast of the former.

Chen et al. (2008c) observed that a total of 1774 aftershocks occurred within one month after the mainshocks. They relocated the two mainshocks and 46 larger aftershocks. Wu et al. (2009) found that the first mainshock is a normal-faulting event caused by the bending of the subducting lithosphere; while the second one is a strike-slip event triggered by the first one.

3.4.10 The Taoyuan Earthquake of 4 March 2008

An earthquake with M_L5.2 was located at (23.20°N,

120.71°E) with H = 11.3 km. The mainshock triggered several hundred aftershocks with $0.4 \le M_L \le 4.8$. From re-located aftershocks, Lin (2010) observed that the major fault plane showed NE-SW-striking and S-E-dipping. From the aftershock spatial distribution, the major fault plane is ~10 km long along the strike and 10 km wide in the dip direction.

Shih et al. (2014) observed that relocated aftershocks formed clusters, and an area with low aftershock activity was beneath the mainshock. The aftershock distribution suggests a southeast-dipping fault plane, which is consistent with one of the nodal planes of the focal-plane solution for the mainshock. Relocated aftershocks are mainly located at the hanging wall side of the mainshock and showed a fault with θ = N37°E and ϕ = 45°SE. They related this earthquake sequence to the Ne-In fault, which is a northern extension of the Chishan fault.

3.4.11 The Jiashian Earthquake of 4 March 2010

An earthquake M_L6.4 was located at (22.97°N, 120.71°E) with H = 22.6 km. Chan and Wu (2012) observed that the seismicity rate in southern Taiwan was significantly higher after than before the mainshock, and the aftershocks decayed following Eq. (2) with k = 100, τ = 63.1 days, and p = 0.74 estimated from the aftershocks with $M_L > 1.7$ and H ≤ 40 km. The results suggest that aftershock activity might last until the end of 2012. Lee et al. (2013a) inferred a complex rupture process with several slip patches distributed inside two main asperities. They also found that most aftershocks occurred near the upper boundary of the deeper asperity and no aftershock was located close to the shallow one.

3.4.12 The Offshore Hualien Earthquake of 31 October 2013

An earthquake with M_L6.7 was located at (23.54°N, 121.39°E) with H = 14.6 km. From relocated events, Xie et al. (2015) observed that the aftershocks occurred to the north of the mainshock and their focal depths increased from west to east.

3.5 Blind Faults Recognized from Spatial Distribution of Aftershocks

A blind fault is an unexposed fault, because it does not cut the ground surface. This type of fault was not paid much attention by geologists and seismologists before it ruptures. Hence, a blind fault can easily cause serious hazards. Damage produced by blind faults was not recognized until the 1989 Loma Prieta, 1992 Landers, and 1994 Northridge earthquakes in California, USA. Hence, the study and identification of a blind fault is important not only for academic interests but also for social needs in seismically active regions, like Taiwan. A blind fault can be recognized from the spatial distribution of a mainshock and its aftershocks (cf. Chen et al. 2010). Some mainshocks, such as the 1973 Tachien, 1976 Wufeng, 1993 Tapu, 1998 Ruey-Li, and 1999 Chi-Yi earthquakes, and their respective aftershocks mentioned above occurred on blind faults.

4. CORRELATIONS BETWEEN MAINSHOCKS AND THE LARGEST AFTERSHOCKS

Studies of the relationships between the mainshock and its aftershocks are significant for understanding the earthquake source rupture processes. For this purpose, it is necessary to set up criteria of space and time windows for selecting reliable aftershocks. According to the relationship between the aftershock area and M_m inferred by Tajima and Kanamori (1985), Wang and Wang (1993) took 100 days and 50 km to be the time and space windows, respectively, for selecting aftershocks. However, their magnitude scales were not uniform: M_H for the events during 1901 - 1978 from Hsu (1971, 1980, 1985), and M_s for those during 1977 - 1991 from the Earthquake Data Report (EDR) of United States Geological Survey (USGS). Nevertheless, their results are acceptable because Wang (1992) stressed that M_H is similar to M_s. Meanwhile, the number of pre-1972 events was small.

Chen and Wang (2012) studied the correlations between mainshocks and their largest aftershocks for Taiwan earthquakes based on a more reliable data set. They took 100 days as the time window for the selection of aftershocks. Since earthquake location is more accurate from local seismic data than from global data, the linear dimension of 50 km is a good space window for the choice of aftershocks. For the purpose of avoiding the loss of some mainshock-aftershock pairs with a distance between their epicenters of being larger than 50 km, they took 100 km to be the space window. Hence, the mainshock from whose epicenter the largest aftershock has a distance of 50 - 100 km is also taken into account. They selected 85 mainshocks ($5.0 \le M_s \le 7.7$) with their individual largest aftershocks from 1973 - 2008 from the data base of the National Earthquake Information Center (NEIC) of USGS. The epicenters and focal depths were taken from the CWB catalog.

We used a data set of 85 events from Chen and Wang (2012) and add 8 mainshocks with their individual largest aftershocks occurring during 2009 - 2015 from the data base of NEIC. Ninety-three event-pairs with $5.0 \le M_s \le 7.7$ were used in this study. The epicenters and focal depths of those events were taken from the CWB catalog. The epicenters of the mainshocks occurred during 1973 - 2008 and those during 2009 - 2015 are shown by open circles and broad open circles, respectively, in Fig. 4. The size of each symbol corresponds to the magnitude of an event: large size for $M_s \ge 7$, moderate size for $6 \le M_s < 7$, and small size for $5 \le M_s < 6$.

Obviously, the number of events is higher in eastern Taiwan than in western Taiwan.

4.1 Correlation between ΔM and M_m

Wang and Wang (1993) obtained an increase in ΔM with M_m as:

$$\Delta M = (-2.97 \pm 1.08) + (0.64 \pm 0.17) M_m \quad (3)$$

Chen and Wang (2012) obtained an increase in ΔM with M_m as:

$$\Delta M = (-0.97 \pm 0.40) + (0.31 \pm 0.07) M_m \quad (4)$$

The plot of ΔM versus M_m for the data used in this work is displayed in Fig. 5. The open and solid circles are made, respectively for the mainshocks occurring before and after 2008. The two symbols are also used in the subsequent figures. Although the data points are scattered, an increase in ΔM with M_m can be delineated. Hence, the regression linear equation of ΔM versus M_m is:

$$\Delta M = (-1.01 \pm 0.39) + (0.31 \pm 0.07) M_m \quad (5)$$

which is shown in Fig. 5 by a broad solid line. Equations (3) and (4) are displayed by a dashed line and a thin solid line, respectively, in Fig. 5. Obviously, Eq. (5) is similar to Eq. (4) and thus the broad and thin solid lines are close to each other.

Equations (3) - (5) all exhibit dependence of ΔM upon M_m as proposed by Sornette and Ouillon (2005). But, the slope value of Eq. (3) is about two times higher than those of Eqs. (4) and (5). This might be due to systematic differences in magnitude scales and numbers of data between the data set used by Wang and Wang (1993) and the other two. The number of data, especially for smaller events, used by Wang and Wang (1993) is smaller than others. Hence, the weighting of larger-sized events in the interference of a regression equation would be higher for Eqs. (4) and (5) than for Eq. (3). An increase in ΔM with M_m is different from Båth's law and the observation made by Utsu (1961). The distributions of data points suggest that there are only low correlations between ΔM and M_m. Hence, each equation cannot be directly applied to predict the magnitude of the largest aftershock from that of its mainshock.

4.2 Difference of Occurrence Times Versus M_m

Wang and Wang (1993) and Chen and Wang (2012) observed that ΔT (T in the unit of day) decreases more or less with M_m. The data points of log(ΔT) versus M_m of this

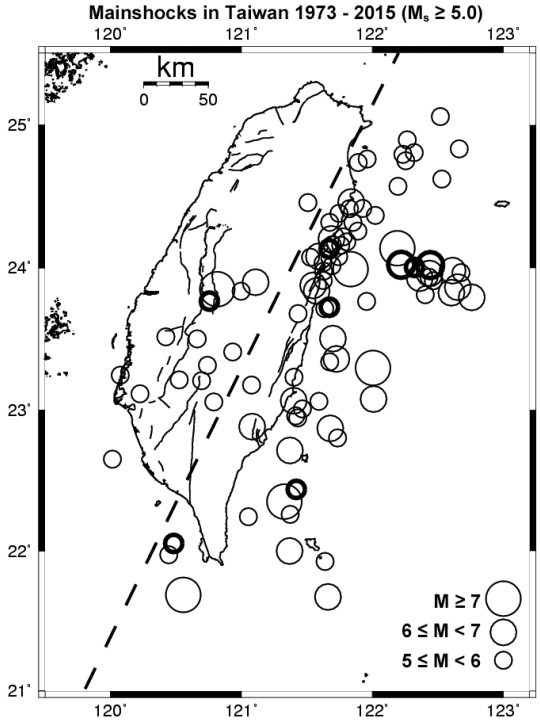

Fig. 4. The epicenters of earthquakes in use are displayed in open circles. The mainshocks occurred after 2008 are plotted by broad open circles. Three kinds of circles with different size denote three magnitude ranges: large size for M ≥ 7, moderate size for 6 ≤ M < 7, and small size for 5 ≤ M < 6. Earthquakes in eastern and western Taiwan are separated by a dashed line.

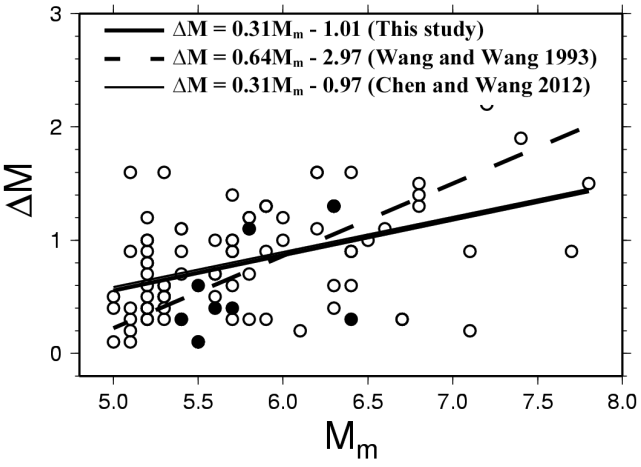

Fig. 5. The plot of ΔM versus M_m. The mainshocks occurred during 1973 - 2008 and those after 2008 are plotted by open circles and solid circles, respectively. The broad solid line represents the regression linear equation of this study: $\Delta M = (-1.01 \pm 0.39) + (0.31 \pm 0.07)M_m$. Includes also are the thin solid line for $\Delta M = (-0.97 \pm 0.40) + (0.31 \pm 0.07)M_m$ inferred by Chen et al. (2012) and the dashed line for $\Delta M = (-2.97 \pm 1.08) + (0.64 \pm 0.17)M_m$ inferred by Wang and Wang (1993).

study are shown in Fig. 6. When $M_m < 6.5$, the data points are in a range of ΔT from 4.2×10^{-3} to 10^2 days, while when $M_m > 6.5$, most of the data points are below 0.83 day.

4.3 Difference of Epicenters Versus M_m

The data points of log(ΔD) (ΔD in the unit of km) versus M_m are demonstrated in Fig. 7. When $M_m < 6.5$, the data points are distributed in a range from 0 - 85 km; while when $M_m > 6.5$, most of the data points are below 35 km. Figure 7 cannot suggest a clear correlation between ΔD and M_m, thus making the location prediction for the largest aftershock from M_m impossible. Nevertheless, results still show that when $M_m > 6.5$ the largest aftershock would occur within an area with a radius being less than 35 km, which is usually the damaged area of the mainshock. This is significant for seismic risk mitigation. The results are similar with those obtained by Chen and Wang (2012).

4.4 Differences of Focal Depths Versus M_m

The data points of log(ΔH) (ΔH in the unit of a kilometer) versus M_m are displayed in Fig. 8. Noted that the aftershock is shallower or deeper than the mainshock when $\Delta H > 0$ or when $\Delta H < 0$, respectively. When $M_m < 6.5$, the data points are in a wider range from -30 to +30 km, while when $M_m > 6.5$, most of them are in a range from -20 to +10 km. Results are similar with those from Chen and Wang. (2012).

Tsapanos (1990) suggested regional-dependence of ΔM. However, Chen and Wang (2012) could not find regional-dependence of ΔM for Taiwan's earthquakes. Since the data set of this study is similar to that used by Chen and Wang (2012), Tsapano's conclusion cannot be confirmed by the present data set.

4.5 Difference of Occurrence Times Versus Difference of Epicenters

Figure 9 shows the plot of log(ΔT) versus log(ΔD). Obviously, the value of ΔT for the open circle is in a big range from few hours to several hundreds of days; while that for the solid circle is longer than 1 day. The figure shows that except for two data points associated with large events, ΔT somewhat increases with ΔD, even though the data points are quite scattered. Hence, it should take a longer time to trigger the largest aftershock due to the mainshock occurrence when the former has a longer distance from the latter. Nevertheless, a correlation between ΔT and ΔD cannot be inferred due to the large scattering of data points. The results are similar to those from Chen and Wang (2012).

5. MAGNITUDE-DEPENDENT P-VALUE

Helmstetter and Sornette (2002) first pointed out the dependence of p-value upon M_m. Ouillon and Sornette (2005) proposed the MSA model from which seismic decay rates after mainshocks follow the Omori's law with a linear increase in the p-value with M_m. Using stacked aftershock sequences of Taiwan in different ranges of M_m, Tsai et al. (2012) inferred an empirical linear relationship $p(M_m) \approx (0.11 \pm 0.01)M_m + (0.38 \pm 0.02)$. Obviously, the p-value is dependent upon M_m, even though the coefficient is small. They also stressed that the coefficients of $p(M_m)$ vary from catalog to catalog and thus do not appear to significantly correlate with any tectonic or structural feature.

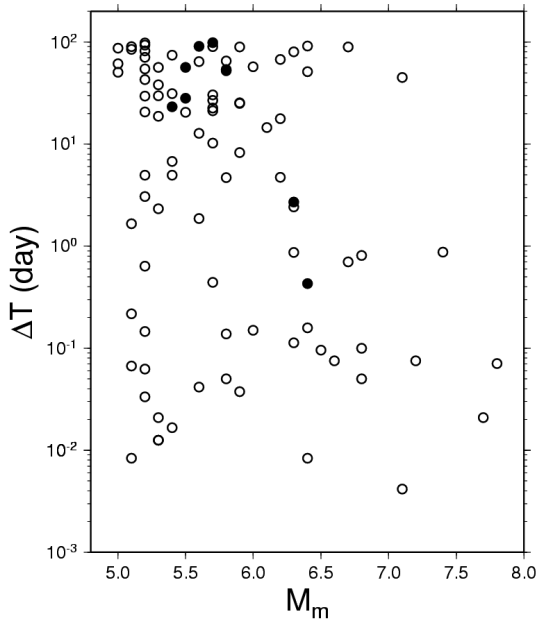

Fig. 6. The plot of log(ΔT) (T in the unit of day) versus M_m. The symbols are the same as those in Fig. 5.

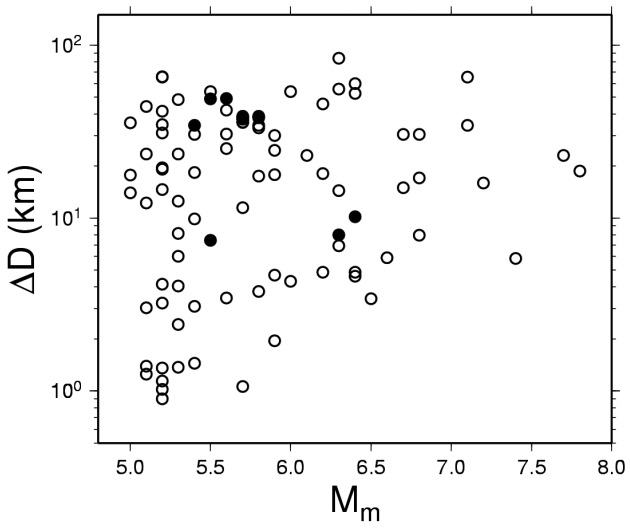

Fig. 7. The plot of log(ΔD) (D in the unit of km) versus M_m. The symbols are the same as those in Fig. 5.

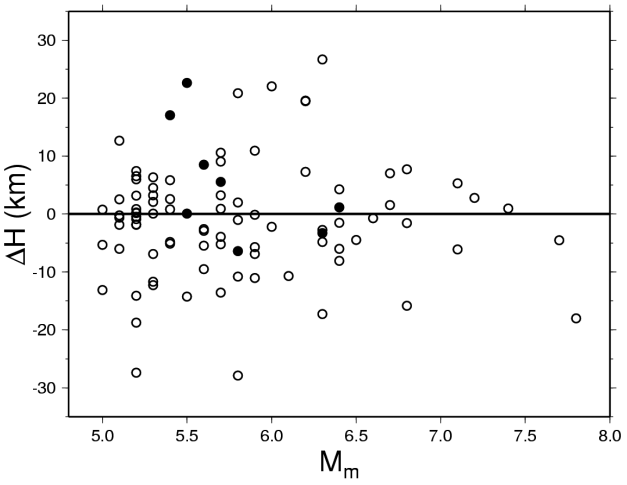

Fig. 8. The plot of log(ΔH) (H in the unit of km) versus M_m. The symbols are the same as those in Fig. 5.

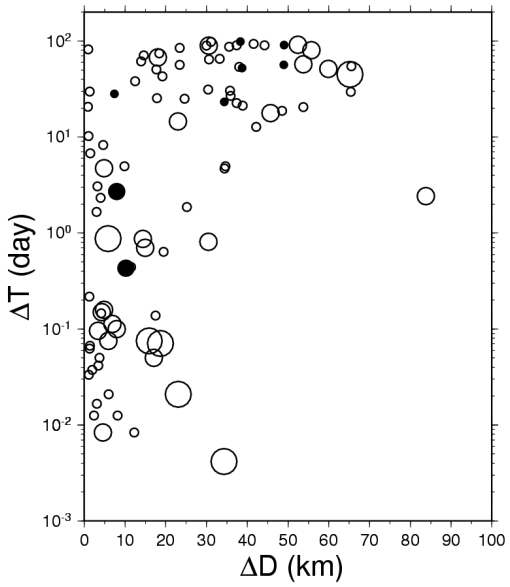

Fig. 9. The plot of log(ΔT) (T in a unit of day) versus log(ΔD) (D in a unit of km). The symbols are the same as those in Fig. 5.

6. CORRELATION BETWEEN b- AND p-VALUES

The b- and the p-values demonstrate the states of fracture and stress of the source area. Hence, the correlation between the two parameters provides a significant constraint for developing a model to interpret aftershock activity. Utsu (1961) assumed that the b- and p-values of an earthquake are positively correlated. However, the data points of b-values versus p-values for Japan's earthquakes in his article form a cluster, and the correlation was not clear. Hence, his assumption is questionable. Yamashita and Knopoff (1987) theoretically derived a positive correlation between b and p-values, especially for the late-occurring aftershocks. Based on the ETAS model, which is based on a universal GR law for all events and an increase in the number of aftershocks with M_m, proposed by Kagan and Knopoff (1981, 1987), Helmstetter and Sornette (2002) presented a positive correlation between b- and p-values. However, the data points for nine large Chinese earthquakes shown in Ma et al. (1992) exhibit a negative correlation between the two parameters. Wang (1994) observed a negative correlation between the two parameters from a larger set of several tens of worldwide earthquakes.

7. APPLICATION OF THE ETAS MODEL TO TAIWAN'S AFTERSHOCKS

Due to the complex foreshocks-mainshock-aftershocks sequence, it is often difficult in classifying an earthquake as a foreshock, a mainshock, or an aftershock. Hence, it is significant to find out a model for which this distinction can be removed and able to study the observations. The ETAS model meets this request and provides a realistic model for aftershocks.

Kawamura and Chen (2013) applied the ETAS model to $M \geq 2.4$ earthquakes of Taiwan. They found seismic quiescence over a broader region of Taiwan. In the inland areas near the epicenter of the Chi-Chi earthquake, seismicity was active from 1 January 1998 to 20 September 1999 before the earthquake. They assumed that this was due to a precursory slip (stress drop) on the earthquake fault plane. This phenomenon is supported by previous studies (e.g., Kato et al. 1997) such as a numerical simulation using rate- and state-dependent friction laws and the observation of abnormal change in crustal displacement for a station of Taiwan GPS network near southern edge of the source area of the Chi-Chi earthquake.

8. AFTERSHOCK TRIGGERING

Aftershocks are assumed to be driven by increases in static Coulomb stress (SCS) on faults near the mainshock caused by fault slip (e.g., King et al. 1994; Stein 1999, 2003). Aftershocks are limited to areas of increased SCS; while the areas of reduced SCS (stress shadows) show low seismicity (Harris and Simpson 1996). However, Ma et al. (2005) and Felzer and Brodsky (2006) found that the SCS changes alone fail to account for the locations of all aftershocks. Aftershocks located at stress shadows could be dynamically triggered by the passage of large-amplitude seismic waves.

Since the occurrence of the 1999 Chi-Chi earthquake, studies on aftershock triggering due to static and dynamic stress changes caused by the mainshock have been made by local seismologists.

8.1 Static Triggering

8.1.1 The Haulien Earthquake of 22 October 1951

Chen et al. (2008a) studied the 1951 Hualien-Taitung

earthquake sequence, including several large earthquakes, which ruptured along four segments of the Taitung Longitudinal Valley fault. This sequence initiated on 21 October 1951 with the M_L7.3 (or M_s7.4) Hualien earthquake followed by a group of M_L6+ aftershocks nearby. They also confirmed aftershock triggering by the mainshock based on the modeled results of SCS changes.

8.1.2 The Chi-Chi Earthquake of 20 September 1999

From the SCS changes caused by the mainshock, Wang (2000) showed that most aftershocks in the fold-and-thrust belt might be triggered by the mainshock. Strike-slip motions near the ends of the Chelungpu fault were also likely to be enhanced by the SCS transfer. Since the Chukou fault was in a stress shadow, few aftershocks occurred there. However, the Chia-Yi earthquake, which occurred a month after the Chi-Chi mainshock, was located at an area without SCS enhancement. He assumed that unless the large aftershocks of the Chi-Chi mainhock altered the stress field and promoted failure, the time lag of the Chia-Yi earthquake might be influenced by a stress shadow.

Wang and Chen (2001) compared the distributions of the SCS changes on the focal nodal planes both before and after the mainshock. Since foreshocks could not be affected by the mainshock, the difference in the distributions indicates the effect of SCS triggering. They found that the SCS change distributions on the Chukou and Meishan faults for events before and after the mainshock were significantly different, yet consistent with the hypothesis of static-stress triggering. They also mentioned that because numerous aftershocks occurred in the stress shadows, other mechanisms, such as dynamic stress, should be taken into account.

Wang et al. (2003) extracted the SCS (permanent) changes from the long-period offsets in the modeled stressgrams due to stress waves generated by the mainshock. They related the calculated SCS changes by the mainshock to seismicity at different depths and over different time intervals to ascertain the stress change effects on aftershock triggering. Results show that correlations between early seismicity rates and SCS changes were low; while correlations between late seismicity rates and SCS changes were much higher. The percentage of early aftershocks at shallow depths (0 - 10 km) in SCS-enhanced areas within 2 weeks after the mainshock was high, yet it decreased considerably at deeper depths (> 10 km) over longer time periods. Hence, SCS changes at depths of 0 - 10 km triggered aftershocks in consideration; while SCS changes at depths might be affected by viscous flow and perturbed by earlier occurred larger aftershocks.

Chan and Ma (2004) studied the relationships between five relocated moderate-large earthquake sequences to the existing faults. The 1993 Da-Pu earthquake resulted from an N-E-striking, W-dipping fault, which cannot be directly confirmed from local geology, and thus it might be attributed to a blind thrust. The rupture of the 1995 Nan-Ao earthquake, which showed an EW-striking, S-dipping fault, might be related to the Lupihsi fault. The 1997 Ruey-Le earthquake showed a NE-SW-striking, E-dipping fault, which might be either the Tachienshan fault or the Chukou fault. The Chia-Yi earthquake rupture showed a NS-striking, W-dipping fault, which cannot be directly confirmed from local geology, and thus it might result from a blind thrust. The aftershock distribution of the Chi-Chi mainshock clearly covered numerous nearby active faults. Hence, the mainshock could trigger the ruptures of nearby active faults including those events.

Ma et al. (2005) compared the percentage of fault planes on which failure occurred after the mainshock relative to the percentage beforehand. Results show a 28% increase for thrust faults and an 18% increase for strike-slip faults. They also observed four lobes with statistically significant decreasing seismicity rates of 40 - 90% for 50 months, and thus the four lobes were coincided with the stress shadows calculated for strike-slip faults.

8.1.3 The Pingtung Offshore Earthquake Doublets of 26 December 2006

Lin et al. (2008) stressed that the second shock and most of their aftershocks were located in a region with an increase in SCS generated by the first shock. They also claimed that the strain energy for each shock had accumulated independently within adjacent crustal volumes, separated by an asperity and the second shock was triggered by the increases in SCS due to the first one.

8.1.4 The Jiashian Earthquake of 4 March 2010

Chan and Wu (2012) observed that most of the consequent events were distributed in the vicinity of a larger-sized earthquake, and large consequent events were located in the regions with SCS increases caused by a previous earthquake. The results confirm interaction between large events. By considering time-dependency, the seismicity rate evolution was estimated based on the rate- and state-dependent friction law. Results suggest that a high seismic rate persisted, at least, until the end of 2012.

8.2 Dynamic Triggering

8.2.1 The Chi-Chi Earthquake of 20 September 1999

Fischer et al. (2008) resolved the continuous signal of acceleration records from the mainshock into a series of relatively short-duration discrete energy bursts through high-frequency band-pass filtering. From these results, they hypothesized that these bursts originated near the individual stations as small, shallow events that were dynamically

triggered by the P- and S-waves generated by the mainshock. Their hypothesis that the bursts are local events is supported by the observation of bursts in the 40-Hz frequency band at distances up to 170 km from the epicenter. Nevertheless, they cannot rule out the possibility that the bursts originated from some non-seismic sources.

Chen et al. (2006) assumed that the bursts originated on the Chelungpu fault plane. This assumption makes the bursts unable be observable at this distance, assuming any reasonable value of crustal attenuation. Based on the local origin, Chen et al. (2006) estimated an average magnitude of M_w0.2 for local events and a source-receiver distance of approximately 1 km. Chen et al. (2006) extended the technique as used by Fischer et al. (2008) to lower stress levels by analyzing records from a smaller (M_w5.3) event. For this event, bursts are observed only on the accelerograms from stations relatively close to the mainshock hypocenter. Analysis of the combined data set from both mainshocks suggests a stress threshold for triggering in the range 0.03 - 0.05 MPa for S-wave triggering and 0.0013 - 0.0033 MPa for P-wave triggering, consistent with prior observations of surface-wave triggering.

9. MODELING OF AFTERSHOCKS

The aftershock triggering mechanisms still remain open. Mogi (1967) first related the power law to a rapid decrease of the stress in the source area immediately after the mainshock. Scholz (1968) assumed that aftershocks are produced by creep rupture due to stress corrosion in stress concentration regions following the mainshock. Harris (2003) summarized the aftershock triggering mechanisms: (1) The pore pressure changes due to pore fluid flows coupled with stress variations, slow redistribution of stress by aseismic creep, rate-and-state dependent friction within faults, coupling between the viscoelastic lower crust and the brittle upper crust, and stress-assisted microcrack corrosion (e.g., Yamashita and Knopoff 1987; Lee and Sornette 2000); (2) Slow tectonic driving of a hierarchical geometry with avalanche relaxation dynamics (e.g., Huang et al. 1998); and (3) The dynamic hierarchical models with heterogeneity, feedbacks, and healing (e.g., Blanter et al. 1997). In addition, Gavrilenko (2005) considered the effect of hydromechaical coupling on aftershocks. Obviously, aftershocks are conventionally considered to be the offspring of the stress alteration in the crust induced by main shocks through some time-dependent processes like pore-fluid flow and viscous relaxation of the lower crust and upper mantle.

Changes in the elastic modulus of materials in terms of the change in stress with strain (cf. Scholz 1990) are widely observed in the experimental stress-stress (or stress-strain) curves, which are also dependent upon temperature. In the low-strain, regime materials generally obey Hooke's law, that is, stress is proportional to strain with a proportional constant, i.e., the Young modulus of elasticity. As strain becomes larger than a certain value, the stress-strain relationships for many materials eventually deviate from the linear one, thus showing anelastic (plastic, ductile, viscoelastic) behavior. Micro-cracks occurring in a material can weaken it when its behavior is deviated from linear elasticity. A continuum approach to the damaging process is thus to introduce an effective Young modulus, which depends on the damage (Turcotte et al. 2003; Shcherbakov and Turcotte 2004b). The mean-field approximation of the microscopic fiber-bundle model suggests that the effective Young modulus decreases from its intact value to zero at the failure of a brittle material.

Chen et al. (2012) considered the decrease in elastic modulus to be a factor in triggering aftershocks. They applied a 1-D N-degree-of-freedom dynamical spring-slider model (Burridge and Knopoff 1967) with varying strengths in elastic modulus as proposed by Wang (1995, 1996) to simulate the spatiotemporal distribution of aftershocks. The generation of aftershocks is due to delayed responses to stress changes induced by the mainshock, that is, the mechanical Maxwell or Kelvin element has to be invoked in the modeling of generating aftershocks. The dashpot in either element produces the viscous effect, thus delaying the response to the induced stress change. Simulation results show spatiotemporal clustering of aftershocks associated with a preceding mainshock. The modified Omori's law with $p \approx 0.8$ holds for the modeled aftershock sequences. They thus suggested that a change of stiffness/strength in materials plays an important role on aftershock triggering. This is different from other models: static and dynamic triggering as mentioned above, fluid effect (e.g., Yamashita 1998, and cited references herein), effect from rate-and-state friction (e.g., Ziv and Rubin 2003, and cited references herein), multifractal stress evolution (e.g., Ouillon and Sornette 2005).

10. SUMMARY

We reviewed the studies on aftershocks in Taiwan for the following topics: the spatial-temporal distributions and focal-plane solutions of aftershocks of some larger-sized earthquakes; interference of the modified Omori law of aftershocks; the correlations between mainshock and the largest aftershock based on the differences in magnitudes, occurrence times, epicenters, and focal depths between mainshocks and their largest aftershocks; magnitude-dependence of p-value of the modified Omori law of aftershocks; the correlation between the b-value of the Gutenberg-Richter's frequency-magnitude law and the p-value; the application of statistical models, for example, the ETAS model, to describe the aftershock sequence; the mechanisms of triggering aftershocks; and dynamic aftershock modeling.

From the studies on aftershocks in Taiwan, several

concluding points can be obtained as described below:

(1) Studies of temporal-spatial distributions and focal-plane solutions for mainshocks and aftershocks of 30 larger Taiwan's earthquakes with magnitudes > 5 show that some mainshocks and their aftershocks are consistent with recognized faults; while others must be described by un-recognized ones, i.e., blind faults. The identification of a blind fault is very important for seismically active regions, like Taiwan. From several examples, the modified Omori's law essentially holds for the aftershock sequences.

(2) The difference in magnitude (ΔM) between the mainshock and the largest aftershock increases with the mainshock magnitude (M_m). Although the data points of ΔM versus M_m are scattered, a correlation between them, with a scaling constant of 0.31, is inferred. However, this correlation cannot be applied to predict the magnitude of the largest aftershock from that of a mainshock. Results are not in agreement with the Båth's law and the observations by Utsu (1961) for Japan's earthquakes.

(3) The dependency of ΔT, which is the difference of occurrence times between the mainshock and the largest aftershock upon M_m is low. This is not good for forecasting the occurrence time of the largest aftershock from that of a mainshock.

(4) The dependence of ΔD, which is the epicentral distance between the main shock and the largest aftershock upon M_m is low.

(5) For all mainshocks examined in this study, ΔT somewhat increases with ΔD. Only considering the mainshocks from which the individual largest aftershocks have a distance of 50 - 100 km, ΔT more or less decreases with increasing ΔD.

(6) There is linear relationship between p-value and M_m for earthquakes in Taiwan: $p(M_m) \approx (0.11 \pm 0.01)M_m + (0.38 \pm 0.02)$.

(7) There is a negative correlation between the b- and p-values from a large set of several tens of worldwide earthquakes. This is inconsistent with theoretical expect by Aki (1981).

(8) Seismic quiescence over a broader region of Taiwan was observed before the 1999 Chi-Chi earthquake, consistent with the ETAS model.

(9) Both static and dynamic stress changes can trigger aftershocks. In the high static-stress-change areas, static triggering works very well; while in the low static-stress-change areas, dynamic triggering must be taken into account.

(10) Dynamic modeling shows that a decrease in elastic modulus is a significant factor in generating aftershocks. This is different from other models.

Acknowledgements The author would like to thank Prof. Ruey-Juin Rau (Editor of Terrestrial, Atmospheric and Oceanic Sciences), Dr. Honn Kao, and the Anonymous Reviewer for their valuable comments and suggestions which substantially improved this article. This study was financially supported by Academia Sinica, the Ministry of Science and Technology (Grand Nos.: MOST 103-2116-M-001-010 and MOST 104-2116-M-001-007), and the Central Weather Bureau (Grand Nos.: MOTC-CWB-104-E-07 and MOTC-CWB-105-E-02), ROC.

REFFERENCES

Aki, K., 1981: A probabilistic synthesis of precursory phenomena. In: Simpson, D. W. and P. G. Richards (Eds.), Earthquake Prediction, American Geophysical Union, Washington, D. C., USA, 566-574, doi: 10.1029/ME004p0566. [Link]

Bak, P. and C. Tang, 1989: Earthquakes as a self-organized critical phenomenon. *J. Geophys. Res.*, **94**, 15635-15637, doi: 10.1029/JB094iB11p15635. [Link]

Båth, M., 1965: Lateral inhomogeneities of the upper mantle. *Tectonophysics*, **2**, 483-514, doi: 10.1016/0040-1951(65)90003-X. [Link]

Båth, M., 1984: A note on Fennoscandian aftershocks. *Boll. Geofis. Teor. Appl.*, **104**, 211-220.

Blanter, E. M., M. G. Shnirman, J. L. Le Mouël, and C. J. Allegre, 1997: Scaling laws in blocks dynamics and dynamic self-organized criticality. *Phys. Earth Planet. Inter.*, **99**, 295-307, doi: 10.1016/S0031-9201(96)03195-0. [Link]

Burridge, R. and L. Knopoff, 1967: Model and theoretical seismicity. *Bull. Seismol. Soc. Am.*, **57**, 341-371.

Chan, C. H. and K. F. Ma, 2004: Association of five moderate-large earthquakes to the faults in Taiwan. *Terr. Atmos. Ocean. Sci.*, **15**, 97-110, doi: 10.3319/TAO.2004.15.1.97(T). [Link]

Chan, C. H. and Y. M. Wu, 2012: A seismicity burst following the 2010 *M* 6.4 Jiashian earthquake – implications for short-term seismic hazards in southern Taiwan. *J. Asian Earth Sci.*, **59**, 231-239, doi: 10.1016/j.jseaes.2012.08.011. [Link]

Chan, C. W. and J. H. Wang, 1990: The error range and P-wave residual to the relocation of earthquakes in the Juisui area during January 1969 to May 1972 by HYPO71 program. *Meteorol. Bull. CWB*, **36**, 305-314. (in Chinese)

Chang, C. H., Y. M. Wu, L. Zhao, and F. T. Wu, 2007: Aftershocks of the 1999 Chi-Chi, Taiwan, earthquake: The first hour. *Bull. Seismol. Soc. Am.*, **97**, 1245-1258, doi: 10.1785/0120060184. [Link]

Chang, J. S. and T. C. Shin, 1994: Earthquakes in 1993. *Meteorol. Bull. CWB*, **39**, 202-217. (in Chinese)

Chen, C. C., W. C. Wang, Y. F. Chang, Y. M. Wu, and Y. H. Lee, 2006: A correlation between the *b*-value and the fractal dimension from the aftershock sequence

of the 1999 Chi-Chi, Taiwan, earthquake. *Geophys. J. Int.*, **167**, 1215-1219, doi: 10.1111/j.1365-246X.2006.03230.x. [Link]

Chen, C. C., J. H. Wang, and W. J. Huang, 2012: Material decoupling as a mechanism of aftershock generation. *Tectonophysics*, **546-547**, 56-59, doi: 10.1016/j.tecto.2012.04.016. [Link]

Chen, K. C. and J. H. Wang, 1984: On the studies of the May 10, 1983 Taipingshan, Taiwan earthquake sequence. *Bull. Inst. Earth Sci. Acad. Sin.*, **4**, 1-27.

Chen, K. C. and J. H. Wang, 1986: The May 20, 1986 Hualien, Taiwan earthquake and its aftershocks. *Bull. Inst. Earth Sci. Acad. Sin.*, **6**, 1-13.

Chen, K. C. and J. H. Wang, 1988: A study on aftershocks and focal mechanisms of two 1986 earthquakes in Hualien, Taiwan. *Proc. Geol. Soc. China*, **31**, 65-72.

Chen, K. C. and J. H. Wang, 2012: Correlations between the mainshock and the largest aftershock for Taiwan earthquakes. *Pure Appl. Geophys.*, **169**, 1217-1229, doi: 10.1007/s00024-011-0352-9. [Link]

Chen, K. C., B. S. Huang, K. L. Wen, H. C. Chiu, Y. T. Yeh, S. N. Cheng, H. Y. Peng, T. M. Chang, T. C. Shin, R. C. Shih, and C. R. Lin, 1999: A study of aftershocks of the 17 July 1998 Ruey-Li, Chiayi earthquake. *Terr. Atmos. Ocean. Sci.*, **10**, 605-618, doi: 10.3319/TAO.1999.10.3.605(T). [Link]

Chen, K. C., B. S. Huang, J. H. Wang, and H. Y. Yen, 2002: Conjugate thrust faulting associated with the 1999 Chi-Chi, Taiwan, earthquake sequence. *Geophys. Res. Lett.*, **29**, doi: 10.1029/2001GL014250. [Link]

Chen, K. C., B. S. Huang, W. G. Huang, J. H. Wang, K. H. Kim, S. J. Lee, Y. C. Lai, S. Tsao, and C. H. Chen, 2010: A blind normal fault beneath the Taipei basin in northern Taiwan. *Terr. Atmos. Ocean. Sci.*, **21**, 495-502, doi: 10.3319/TAO.2010.01.25.01(TH). [Link]

Chen, K. H., S. Toda, and R. J. Rau, 2008a: A leaping, triggered sequence along a segmented fault: The 1951 M_L 7.3 Hualien-Taitung earthquake sequence in eastern Taiwan. *J. Geophys. Res.*, **113**, B02304, doi: 10.1029/2007JB005048. [Link]

Chen, X., D. Yuan, and C. Wu, 1996: Characteristics of ruptures of M_s7.3 earthquake in the Taiwan Strait and analysis of seismicity in the off-shore Southeastern area. *Acta Seism. Sin.*, **18**, 145-155. (in Chinese)

Chen, Y. G., Y. T. Kuo, Y. M. Wu, H. L. Chen, C. H. Chang, R. Y. Chen, P. W. Lo, K. E. Ching, and J. C. Lee, 2008b: New seismogenic source and deep structures revealed by the 1999 Chia-yi earthquake sequence in southwestern Taiwan. *Geophys. J. Int.*, **172**, 1049-1054, doi: 10.1111/j.1365-246X.2007.03686.x. [Link]

Chen, Y. R., Y. C. Lai, Y. L. Huang, B. S. Huang, and K. L. Wen, 2008c: Investigation of source depths of the 2006 Pingtung earthquake sequence using a dense array at teleseismic distances. *Terr. Atmos. Ocean. Sci.*, **19**, 579-588, doi: 10.3319/TAO.2008.19.6.579(PT). [Link]

Cheng, S. N., B. S. Huang, and Y. T. Yeh, 1996: A study of the 1941 Chungpu, Chiayi, earthquake sequence. Proc. 6th Taiwan Symp. Geophys., 47-56. (in Chinese)

Chiang, S. T., Y. B. Tsai, and J. H. Wang, 1986: Relocation of main aftershocks of April 24, 1972 Juisui earthquakes. Proc. Taiwan Symp. Geophys., 61-74.

Chou, N. P. and J. H. Wang, 1992: A study on source rupture of the 1978 Lan-Hsu, southeastern Taiwan earthquake. *Terr. Atmos. Ocean. Sci.*, **3**, 1-20, doi: 10.3319/TAO.1992.3.1.1(T). [Link]

Felzer, K. R. and E. E. Brodsky, 2006: Decay of aftershock density with distance indicates triggering by dynamic stress. *Nature*, **441**, 735-738, doi: 10.1038/nature04799. [Link]

Fischer, A. D., C. G. Sammis, Y. Chen, and T. L. Teng, 2008: Dynamic triggering by strong-motion *P* and *S* Waves: Evidence from the 1999 Chi-Chi, Taiwan, earthquake. *Bull. Seismol. Soc. Am.*, **98**, 580-592, doi: 10.1785/0120070155. [Link]

Freed, A. M., 2005: Earthquake triggering by static, dynamic, and postseismic stress transfer. *Annu. Rev. Earth Planet. Sci.*, **33**, 335-367, doi: 10.1146/annurev.earth.33.092203.122505. [Link]

Gardner, J. K. and L. Knopoff, 1974: Is the sequence of earthquakes in Southern California, with aftershocks removed, Poissonian? *Bull. Seismol. Soc. Am.*, **64**, 1363-1367.

Gavrilenko, P., 2005: Hydromechanical coupling in response to earthquakes: On the possible consequences for aftershocks. *Geophys. J. Int.*, **161**, 113-129, doi: 10.1111/j.1365-246X.2005.02538.x. [Link]

Gutenberg, B. and C. F. Richter, 1944: Frequency of earthquakes in California. *Bull. Seismol. Soc. Am.*, **34**, 185-188.

Harris, R. A., 2003: Stress triggers, stress shadows, and seismic hazard. In: Lee, W. H. K., H. Kanamori, P. C. Jennings, and C. Kisslinger (Eds.), International Handbook of Earthquake and Engineering Seismology, Part B, Chapter 73, Academic Press, 1217-1232, doi: 10.1016/S0074-6142(03)80187-0. [Link]

Harris, R. A. and R. W. Simpson, 1996: In the shadow of 1857-the effect of the great Ft. Tejon earthquake on subsequent earthquakes in southern California. *Geophys. Res. Lett.*, **23**, 229-232, doi: 10.1029/96GL00015. [Link]

Helmstetter, A. and D. Sornette, 2002: Subcritical and supercritical regimes in epidemic models of earthquake aftershocks. *J. Geophys. Res.*, **107**, doi: 10.1029/2001JB001580. [Link]

Helmstetter, A. and D. Sornette, 2003: Båth's law derived from the Gutenberg-Richter law and from aftershock properties. *Geophys. Res. Lett.*, **30**, doi:

10.1029/2003GL018186. [Link]

Hirata, T., 1987: Omori's Power Law aftershock sequences of microfracturing in rock fracture experiment. *J. Geophys. Res.*, **92**, 6215-6221, doi: 10.1029/JB092iB07p06215. [Link]

Hirata, T., 1989: A correlation between the *b* value and the fractal dimension of earthquakes. *J. Geophys. Res.*, **94**, 7507-7514, doi: 10.1029/JB094iB06p07507. [Link]

Hsu, H., 1983: Source materials on the history of natural disasters in Ching Taiwan. Hazards Mitigation S&T Report, Vol. 72-01, 5-6. (in Chinese).

Hsu, M. T., 1971: Seismicity of Taiwan and some related problems. *Bull. Int. I. Seismol. Earthq. Eng.*, **8**, 41-160.

Hsu, M. T., 1980: Earthquake Catalog in Taiwan (from 1644 to 1979). Earthquake Engin. Res. Center, Taiwan Univ., 77 pp. (in Chinese)

Hsu, M. T., 1985: Computation of magnitudes of earthquakes occurred in 1934 and 1935. *Meteorol. Bull.*, **31**, 103-106. (in Chinese)

Hsu, M. T. and H. M. Lu, 1969: Report on Tainan Chiayi earthquake of Jan. 18, 1964. Open File Rept., Taiwan Weather Bureau, 55 pp. (in Chinese)

Huang, B. S. and Y. T. Yeh, 1992: Source geometry and slip distribution of the April 21, 1935 Hsinchu-Taichung, Taiwan earthquake. *Tectonophysics*, **210**, 77-90, doi: 10.1016/0040-1951(92)90129-T. [Link]

Huang, M. W. and J. H. Wang, 2002: Scaling of displacement spectra of near-fault seismograms of the 1999 Chi-Chi, Taiwan, earthquake. *Geophys. Res. Lett.*, **29**, doi: 10.1029/2001GL014021. [Link]

Huang, M. W. and J. H. Wang, 2009: Scaled energies of $M_L \geq 5.1$ aftershocks of the 1999 Chi-Chi, Taiwan, earthquake measured from local seismograms. *Terr. Atmos. Ocean. Sci.*, **20**, 671-685, doi: 10.3319/TAO.2008.10.13.01(T). [Link]

Huang, M. W., J. H. Wang, R. D. Hwang, and K. C. Chen, 2002: Estimates of source parameters of two large aftershocks of the 1999 Chi-Chi, Taiwan, earthquake in the Chia-Yi area. *Terr. Atmos. Ocean. Sci.*, **13**, 299-312, doi: 10.3319/TAO.2002.13.3.299(CCE). [Link]

Huang, M. W., J. H. Wang, H. H. Hsieh, K. L. Wen, and K. F. Ma, 2005: Frequency-dependent sites amplifications evaluated from well-logging data in central Taiwan. *Geophys. Res. Lett.*, **32**, L21302, doi: 10.1029/2005GL023527. [Link]

Huang, Y., H. Saleur, C. Sammis, and D. Sornette, 1998: Precursors, aftershocks, criticality and self-organized criticality. *Europhys. Lett.*, **41**, 43-48.

Kagan, Y. Y. and L. Knopoff, 1981: Stochastic synthesis of earthquake catalogs. *J. Geophys. Res.*, **86**, 2853-2862, doi: 10.1029/JB086iB04p02853. [Link]

Kagan, Y. Y. and L. Knopoff, 1987: Statistical short-term earthquake prediction. *Science*, **236**, 1563-1567, doi: 10.1126/science.236.4808.1563. [Link]

Kao, H. and W. P. Chen, 2000: The Chi-Chi earthquake sequence: Active, out-of-sequence thrust faulting in Taiwan. *Science*, **288**, 2346-2349, doi: 10.1126/science.288.5475.2346. [Link]

Kao, H. and F. T. Wu, 1996: The 16 September 1994 earthquake (m_b=6.5) in the Taiwan Strait and its tectonic implications. *Terr. Atmos. Ocean. Sci.*, **7**, 13-29, doi: 10.3319/TAO.1996.7.1.13(T). [Link]

Kato, N., M. Ohtake, and T. Hirasawa, 1997: Possible mechanism of precursory seismic quiescence: Regional stress relaxation due to preseismic sliding. *Pure Appl. Geophys.*, **150**, 249-267, doi: 10.1007/s000240050075. [Link]

Kawamura, M. and C. Chen, 2013: Precursory change in seismicity revealed by the Epidemic-Type Aftershock-Sequences model: A case study of the 1999 Chi-Chi, Taiwan earthquake. *Tectonophysics*, **592**, 141-149, doi: 10.1016/j.tecto.2013.02.017. [Link]

Kawasumi, H. and S. Honma, 1936: On a problem concerning the internal structure of the Earth as discussed from the time-distance curve of the Formosa earthquake of April 20, 1935. *Bull. Earthq. Res. Inst. Tokyo Imperial University*, **3**, 10-21.

Kilb, D., J. Gomberg, and P. Bodin, 2000: Triggering of earthquake aftershocks by dynamic stresses. *Nature*, **408**, 570-574, doi: 10.1038/35046046. [Link]

Kim, K. H., K. C. Chen, J. H. Wang, and J. M. Chiu, 2010: Seismogenic structures of the 1999 M_w7.6 Chi-Chi, Taiwan, earthquake and its aftershocks. *Tectonophysics*, **489**, 119-127, doi: 10.1016/j.tecto.2010.04.011. [Link]

King, G. C. P., R. S. Stein, and J. Lin, 1994: Static stress changes and the triggering of earthquakes. *Bull. Seismol. Soc. Am.*, **84**, 935-953.

Knopoff, L., Y. Y. Kagan, and R. Knopoff, 1982: *b* values for foreshocks and aftershocks in real and simulated earthquake sequences. *Bull. Seismol. Soc. Am.*, **72**, 1663-1676.

Kuo, K. W., T. C. Shin, and C. H. Chang, 1994: The December 16, 1993 Tapu earthquake. *Meteorol. Bull.*, **39**, 125-131. (in Chinese)

Kuochen, H., Y. M. Wu, Y. G. Chen, and R. Y. Chen, 2007: 2003 Mw6.8 Chengkung earthquake and its related seismogenic structures. *J. Asian Earth Sci.*, **31**, 332-339, doi: 10.1016/j.jseaes.2006.07.028. [Link]

Lee, M. W. and D. Sornette, 2000: Novel mechanism for discrete scale invariance in sandpile models. *Eur. Phys. J. B*, **15**, 193-197, doi: 10.1007/s100510051115. [Link]

Lee, P. H., 1985: The seismic network of the Central Weather Bureau. Proc. Seminar Commem. 50th Anniv. for Hsinchu-Taichung Earthquake of 1935, 114-123. (in Chinese)

Lee, P. H, Y. L. Liu, K. T. Chen, and J. W. Chan, 1985:

Relocation of the 1935 earthquake sequence. Proc. Seminar Commem. 50th Anniv. for Hsinchu-Taichung Earthquake of 1935, 59-67. (in Chinese)

Lee, S. J., L. Mozziconacci, W. T. Liang, Y. J. Hsu, W. G. Huang, and B. S. Huang, 2013a: Source complexity of the 4 March 2010 Jiashian, Taiwan, Earthquake determined by joint inversion of teleseismic and near field data. *J. Asian Earth Sci.*, **64**, 14-26, doi: 10.1016/j.jseaes.2012.11.018. [Link]

Lee, T. Q. and Y. B. Tsai, 1981: A study of the July 23, 1978 Lanhsu, Taiwan earthquake sequence. *Bull. Inst. Earth Sci. Acad. Sin.*, **1**, 31-50.

Lee, Y. T., D. L. Turcotte, J. B. Rundle, and C. C. Chen, 2013b: Aftershock statistics of the 1999 Chi-Chi, Taiwan earthquake and the concept of Omori times. *Pure Appl. Geophys.*, **170**, 221-228, doi: 10.1007/s00024-011-0445-5. [Link]

Lennartz, S., A. Bunde, and D. L. Turcotte, 2011: Modelling seismic catalogues by cascade models: Do we need long-term magnitude correlations? *Geophys. J. Int.*, **184**, 1214-1222, doi: 10.1111/j.1365-246X.2010.04902.x. [Link]

Liaw, Z. S., C. Wang, and Y. T. Yeh, 1986: A study of aftershocks of the 20 May 1986 Hualien earthquake. *Bull. Inst. Earth Sci. Acad. Sin.*, **6**, 15-27.

Lin, C. H., 2002: Active continental subduction and crustal exhumation: The Taiwan orogeny. *Terra Nova*, **14**, 281-287.

Lin, C. H., 2010: Temporal *b*-value variations throughout a seismic faulting process: The 2008 Taoyuan earthquake in Taiwan. *Terr. Atmos. Ocean. Sci.*, **21**, 229-234, doi: 10.3319/TAO.2009.02.09.01(T). [Link]

Lin, C. H., Y. H. Yeh, M. Ando, K. J. Chen, T. M. Chang, and H. C. Pu, 2008: Earthquake doublet sequences: Evidence of static triggering in the strong convergent zones of Taiwan. *Terr. Atmos. Ocean. Sci.*, **19**, 589-594, doi: 10.3319/TAO.2008.19.6.589(PT). [Link]

Liu, K. S., T. C. Shin, and Y. B. Tsai, 1999: A free-field strong motion network in Taiwan: TSMIP. *Terr. Atmos. Ocean. Sci.*, **10**, 337-396, doi: 10.3319/TAO.1999.10.2.377(T). [Link]

Lu, C. P., 1974: Implications from aftershocks of Tachien earthquake of 24 December 1973. Annual Report of the Institute of Physics, Academia Sinica, 1973-IESEP-005, IESAS5, 305-325.

Lu, S. M., 1960: Report on Hengchun Earthquake of Aug. 15, 1959, Open File Report, Taiwan Weather Bureau, 65 pp. (in Chinese)

Lu, S. M., Y. J. Hsu, and N. Shih, 1976: Report on Jui-Sui Earthquake of Hwalien Hsien 24 April, 1972, Open File Report, Central Weather Bureau, 82 pp. (in Chinese)

Ma, K. F. and J. Y. Chen, 1999: Focal mechanism determinations of the 1991 Chiali earthquake (M_L=5.7) sequence. *Terr. Atmos. Ocean. Sci.*, **10**, 447-470, doi: 10.3319/TAO.1999.10.2.447(T). [Link]

Ma, K. F., C. T. Lee, Y. B. Tsai, T. C. Shin, and J. Mori, 1999: The Chi-Chi, Taiwan earthquake: Large surface displacements on an inland thrust fault. *Eos, Trans., AGU*, **80**, 605-611, doi: 10.1029/99EO00405. [Link]

Ma, K. F., C. H. Chan, and R. S. Stein, 2005: Response of seismicity to Coulomb stress triggers and shadows of the 1999 M_w = 7.6 Chi-Chi, Taiwan, earthquake. *J. Geophys. Res.*, **110**, B05S19, doi: 10.1029/2004JB003389. [Link]

Ma, Z., X. Li, and J. Jin, 1992: The law interpretation and prediction of earthquake migration-Earthquake Migration of four seismic belts in China Mainland. *Seismology and Geology*, **14**, 129-139. (in Chinese)

Main, I. G., P. G. Meredith, and P. R. Sammonds, 1992: Temporal variations in seismic event rate and *b*-values from stress corrosion constitutive laws. *Tectonophysics*, **211**, 233-246, doi: 10.1016/0040-1951(92)90061-A. [Link]

Mandelbrot, B. B., 1982: The Fractal Geometry of Nature, W. H. Freeman and Company, San Francisco, CA, USA, 468 pp.

Meyer, S. L., 1975: Data Analysis for Scientists and Engineers, John Wiley & Dons, New York, 513 pp.

Miyatake, T., 1985: Earthquake source process and aftershock activity. *Zisin*, **38**, 67-79. (in Japanese)

Mogi, K., 1962: Study of elastic shocks caused by the fracture of heterogeneous materials and its relations to earthquake phenomena. *Bull. Earthq. Res. Inst.*, **40**, 125-173.

Mogi, K., 1967: Regional variations in magnitude-frequency relation of earthquakes. *Bull. Earthq. Res. Inst.*, **45**, 313-325.

Molchan, G. M. and O. E. Dmitrieva, 1992: Aftershock identification: Methods and new approaches. *Geophys. J. Int.*, **109**, 501-516, doi: 10.1111/j.1365-246X.1992.tb00113.x. [Link]

Nakamura, S., 1922: On the destructive earthquakes in Formosa on the 2nd and 15th of September, 1922. *Seismol. Bull., Central Meteorol. Obser.*, **1**, 60-69.

Nasu, N., 1936a: The aftershocks of the Formosa earthquake of 1935. *Bull. Earthq. Res. Inst. Tokyo University*, **3**, 75-89. (in Japanese)

Nasu, N., 1936b: On aftershocks of the 1935 Formosa earthquake. *Zisin*, **8**, 57-67. (in Japanese)

Ogata, Y., 1988: Statistical models for earthquake occurrences and residual analysis for point processes. *J. Am. Stat. Assoc.*, **83**, 9-27, doi: 10.1080/01621459.1988.10478560. [Link]

Omori, F., 1894a: On the aftershocks of earthquakes. *J. Coll. Sci., Imp. Univ. Tokyo*, **7**, 111-120.

Omori, F., 1894b: On the aftershocks. *Rep. Imp. Earthquake Inv Comm.*, **2**, 103-139.

Omori, F., 1907a: Preliminary note on the Formosa earthquake of March 17, 1906. *Bull. Imp. Earthquake Invest. Comm.*, **1**, 53-69.

Omori, F., 1907b: Comparison of the faults in the three earthquakes of Mino-Owari, Formosa and San Francisco. *Bull. Imp. Earthquake Invest. Comm.*, **1**, 70-72.

Omori, F., 1908: Earthquake distribution in Formosa. *Bull. Imp. Earthquake Invest. Comm.*, **2**, 148-155.

Ouillon, G. and D. Sornette, 2005: Magnitude-dependent Omori law: Theory and empirical study. *J. Geophys. Res.*, **110**, B04306, doi: 10.1029/2004JB003311. [Link]

Reasenberg, P. A. and L. M. Jones, 1989: Earthquake hazard after a mainshock in California. *Science*, **243**, 1173-1176, doi: 10.1126/science.243.4895.1173. [Link]

Scholz, C. H., 1968: Microfractures, aftershocks, and seismicity. *Bull. Seismol. Soc. Am.*, **58**, 1117-1130.

Scholz, C. H., 1990: The Mechanics of Earthquakes and Faulting, Cambridge University Press, 461 pp.

Shaw, B. E., 1993: Generalized Omori law for aftershocks and foreshocks from a simple dynamics. *Geophys. Res. Lett.*, **20**, 907-910, doi: 10.1029/93GL01058. [Link]

Shcherbakov, R. and D. L. Turcotte, 2004: A damage mechanics model for aftershocks. *Pure Appl. Geophys.*, **161**, 2379-2391, doi: 10.1007/s00024-004-2570-x. [Link]

Shearer, P. M., 2012: Self-similar earthquake triggering, Båth's law, and foreshock/aftershock magnitudes: Simulations, theory, and results for southern California. *J. Geophys. Res.*, **117**, B06310, doi: 10.1029/2011JB008957. [Link]

Shebalin, P. N. and V. I. Keilis-Borok, 1999: Phenomenon of local 'seismic reversal' before strong earthquakes. *Phys. Earth Planet. Inter.*, **111**, 215-227, doi: 10.1016/S0031-9201(98)00162-9. [Link]

Sheu, H. C., M. Kosuga, and H. Sato, 1982: Mechanism and fault model of the Hsinchu-Taichung (Taiwan) earthquake of 1935. *Seismol. Soc. Japan Jour.*, **35**, 567-574. (in Japanese)

Shih, M. H., B. S. Huang, L. Zhu, H. Y. Yen, T. M. Chang, W. G. Huang, and C. Y. Wang, 2014: Fault orientation determination for the 4 March 2008 Taoyuan earthquake from dense near-source seismic observations. *Terr. Atmos. Ocean. Sci.*, **25**, 637-645, doi: 10.3319/TAO.2014.05.19.01(T). [Link]

Shin, T. C., 1992: Some implications of Taiwan tectonic features from the data collected by the Central Weather Bureau Seismic Network. *Meteorol. Bull. CWB*, **38**, 23-48. (in Chinese)

Shin, T. C., 1993: The calculation of local magnitude from the simulated Wood-Anderson seismograms of the short-period seismograms in the Taiwan area. *Terr. Atmos. Ocean. Sci.*, **4**, 155-170, doi: 10.3319/TAO.1993.4.2.155(T). [Link]

Shin, T. C., 1995: Application of waveform modeling to determine focal mechanisms of the 1993 Tapu earthquake and its aftershocks. *Terr. Atmos. Ocean. Sci.*, **6**, 167-179, doi: 10.3319/TAO.1995.6.2.167(T). [Link]

Shin, T. C. and J. S. Chang, 1992: Earthquakes in 1992. *Meteorol. Bull. CWB*, **38**, 218-232.

Shin, T. C. and J. S. Chang, 2005: Earthquake monitoring systems in Taiwan. In: Wang, J. H. (Ed.), The 921 Chi-Chi Major Earthquake, Office of Inter-Ministry Science and Technology Program for Earthquake and Active-fault Research, NSC, 43-59. (in Chinese)

Shin, T. C. and T. L. Teng, 2001: An overview of the 1999 Chi-Chi, Taiwan, earthquake. *Bull. Seismol. Soc. Am.*, **91**, 895-913, doi: 10.1785/0120000738. [Link]

Shin, T. C., C. H. Chang, and C. H. Ching, 1994: The March 1991 Chia-li earthquake sequence. *Meteorol. Bull. CWB*, **40**, 17-36. (in Chinese)

Sornette, D. and G. Ouillon, 2005: Multifractal scaling of thermally activated rupture processes. *Phys. Rev. Lett.*, **94**, 038501, doi: 10.1103/PhysRevLett.94.038501. [Link]

Stein, R. S., 1999: The role of stress transfer in earthquake occurrence. *Nature*, **402**, 605-609, doi: 10.1038/45144. [Link]

Stein, R. S., 2003: Earthquake conversations. *Sci. Am.*, **288**, 72-79.

Su, C. Y., 1985: A study on the great eastern Taiwan earthquakes of 1951 and the distribution of great earthquakes in Taiwan. *Bull. Int. Inst. Seismol. Earthq. Eng.*, **21**, 177-194.

Tajima, F. and H. Kanamori, 1985: Global survey of aftershock area expansion patterns. *Phys. Earth Planet. Inter.*, **40**, 77-134, doi: 10.1016/0031-9201(85)90066-4. [Link]

Tsai, C. Y., G. Ouillon, and D. Sornette, 2012: New empirical tests of the multifractal Omori Law for Taiwan. *Bull. Seismol. Soc. Am.*, **102**, 2128-2138, doi: 10.1785/0120110237. [Link]

Tsai, Y. B., T. L. Teng, J. M. Chiu, and H. L. Liu, 1977: Tectonic implications of the seismicity in the Taiwan region. *Mem. Geol. Soc. China*, **2**, 13-41.

Tsapanos, T. M., 1990: Spatial distribution of the difference between the magnitudes of the main shock and the largest aftershock in the circum-Pacific belt. *Bull. Seismol. Soc. Am.*, **80**, 1180-1189.

Turcotte, D. L., 1997: Fractals and Chaos in Geology and Geophysics, Cambridge University Press, Cambridge, UK, 416 pp.

Turcotte, D. L., W. I. Newman, and R. Shcherbakov, 2003: Micro and macroscopic models of rock fracture. *Geophys. J. Int.*, **152**, 718-728, doi: 10.1046/j.1365-246-X.2003.01884.x. [Link]

Utsu, T., 1957: Magnitude of earthquakes and occurrence of their aftershocks. *Zisin*, **10**, 35-45.

Utsu, T., 1961: A statistical study on the occurrence of aftershocks. *Geophys. Mag.*, **30**, 521-605.

Utsu, T., Y. Ogata, and R. S. Matsu'ura, 1995: The centenary of the Omori law for a decay law of aftershock activity. *J. Phys. Earth*, **43**, 1-33, doi: 10.4294/jpe1952.43.1. [Link]

Wang, C., Y. M. Wu, C. F. Chang, A. T. Chen, Y. L. Liu, and W. F. Chien, 1992a: A study of the tectonic cause of 1972 Juisui earthquake in eastern Taiwan. *Meteorol. Bull.*, **38**, 14-22. (in Chinese)

Wang, C., C. F. Chang, T. C. Shin, Y. L. Liu, and C. H. Jian, 1992b: A study of distribution and cause of earthquakes in the Hualien area. *Meteorol. Bull.*, **38**, 203-217. (in Chinese)

Wang, C. T. and J. H. Wang, 1993: Aspects of large Taiwan earthquakes and their aftershocks. *Terr. Atmos. Ocean. Sci.*, **4**, 257-271, doi: 10.3319/TAO.1993.4.3.257(T). [Link]

Wang, C. Y. and T. C. Shin, 1998: Illustrating 100 years of Taiwan seismicity. *Terr. Atmos. Ocean. Sci.*, **9**, 589-614, doi: 10.3319/TAO.1998.9.4.589(T). [Link]

Wang, J. C., C. F. Shieh, and T. M. Chang, 2003: Static stress changes as a triggering mechanism of a shallow earthquake: Case study of the 1999 Chi-Chi (Taiwan) earthquake. *Phys. Earth Planet. Inter.*, **135**, 17-25, doi: 10.1016/S0031-9201(02)00175-9. [Link]

Wang, J. C., J. H. Wang, C. F. Shieh, and Y. H. Yeh, 2010: Static stress transfer between the Chinshan and Shanchiao faults in the Taipei metropolitan area. *Terr. Atmos. Ocean. Sci.*, **21**, 515-527, doi: 10.3319/TAO.2009.11.24.01(TH). [Link]

Wang, J. C., C. F. Shieh, and J. H. Wang, 2013: A study of interactions between thrust and strike-slip faults. *Terr. Atmos. Ocean. Sci.*, **24**, 809-825, doi: 10.3319/TAO.2013.05.08.02(T). [Link]

Wang, J. H., 1988: *b* values of shallow earthquakes in Taiwan. *Bull. Seismol. Soc. Am.*, **78**, 1243-1254.

Wang, J. H., 1989: The Taiwan Telemetered Seismographic Network. *Phys. Earth Planet. Inter.*, **58**, 9-18, doi: 10.1016/0031-9201(89)90090-3. [Link]

Wang, J. H., 1992: Magnitude scales and their relations for Taiwan earthquakes: A review. *Terr. Atmos. Ocean. Sci.*, **3**, 449-468, doi: 10.3319/TAO.1992.3.4.449(T). [Link]

Wang, J. H., 1994: On the correlation of observed Gutenberg-Richter's *b* value and Omori's *p* value for aftershocks. *Bull. Seismol. Soc. Am.*, **84**, 2008-2011.

Wang, J. H., 1995: Effect of seismic coupling on the scaling of seismicity. *Geophys. J. Int.*, **121**, 475-488, doi: 10.1111/j.1365-246X.1995.tb05727.x. [Link]

Wang, J. H., 1996: Velocity-weakening friction as a factor in controlling the frequency-magnitude relation of earthquakes. *Bull. Seismol. Soc. Am.*, **86**, 701-713.

Wang, J. H., 1998: Studies of earthquake seismology in Taiwan during the 1897-1996 period. *J. Geol. Soc. China*, **41**, 291-336.

Wang, J. H., 2008: Urban seismology in the Taipei Metropolitan Area: Review and prospective. *Terr. Atmos. Ocean. Sci.*, **19**, 213-233, doi: 10.3319/TAO.2008.19.3.213(T). [Link]

Wang, J. H., 2013: Memory effect in $M \geq 6$ earthquakes of South-North Seismic Belt, Mainland China. *J. Seismol.*, **17**, 913-924, doi: 10.1007/s10950-013-9361-8. [Link]

Wang, J. H., 2014: Memory effect in $M \geq 7$ earthquakes of Taiwan. *J. Seismol.*, **18**, 467-480, doi: 10.1007/s10950-014-9420-9. [Link]

Wang, J. H. and M. W. Huang, 2007: Effect of finite frequency bandwidth limitation on evaluations of seismic radiation energy of the 1999 Chi-Chi earthquake. *Terr. Atmos. Ocean. Sci.*, **18**, 567-576, doi: 10.3319/TAO.2007.18.3.567(T). [Link]

Wang, J. H. and C. W. Lee, 1996: Multifractal measures of earthquakes in west Taiwan. *Pure Appl. Geophys.*, **146**, 131-145, doi: 10.1007/BF00876673. [Link]

Wang, J. H. and C. W. Lee, 1997: Multifractal measures of time series of earthquakes. *J. Phys. Earth*, **45**, 331-345, doi: 10.4294/jpe1952.45.331. [Link]

Wang, J. H., T. L. Teng and K. F. Ma, 1989: Temporal variation of coda *Q* during Hualien earthquake of 1986 in eastern Taiwan. *Pure Appl. Geophys.*, **130**, 617-634, doi: 10.1007/BF00881601. [Link]

Wang, J. H., C. Y. Wang, Q. C. Song, T. C. Shin, S. B. Yu, C. F. Shieh, K. L. Wen, S. L. Chung, M. Lee, K. M. Kuo, and K. C. Chang, 2005: The 921 Chi- Chi Major Earthquake, Office of Inter-Ministry Science & Technology Program for Earthquake and Active-fault Research, National Science Council, 582 pp. (in Chinese)

Wang, W. H., 2000: Static stress transfer and aftershock triggering by the 1999 Chi-Chi earthquake in Taiwan. *Terr. Atmos. Ocean. Sci.*, **11**, 631-642, doi: 10.3319/TAO.2000.11.3.631(CCE). [Link]

Wang, W. H. and C. H. Chen, 2001: Static stress transferred by the 1999 Chi-Chi, Taiwan, earthquake: Effects on the stability of the surrounding fault systems and aftershock triggering with a 3D fault-slip model. *Bull. Seismol. Soc. Am.*, **91**, 1041-1052, doi: 10.1785/0120000727. [Link]

Wu, F. T., 1978: Recent tectonics of Taiwan. *J. Phys. Earth*, **26**, S265-S299, doi: 10.4294/jpe1952.26.Supplement_S265. [Link]

Wu, Y. M. and C. Chen, 2007: Seismic reversal pattern for the 1999 Chi-Chi, Taiwan, M_W 7.6 earthquake. *Tectonophysics*, **429**, 125-132, doi: 10.1016/j.tecto.2006.09.015. [Link]

Wu, Y. M., L. Zhao, C. H. Chang, N. C. Hsiao, Y. G. Chen, and S. K. Hsu, 2009: Relocation of the 2006 Pingtung Earthquake sequence and seismotectonics in Southern

Taiwan. *Tectonophysics*, **479**, 19-27, doi: 10.1016/j.tecto.2008.12.001. [Link]

Xie, X., J. Sun, Z. Xie, S. Xia, J. Cao, K. Wan, and H. Xu, 2015: Source parameters of 31 October 2013 Hualien earthquake of Longitudinal Valley in eastern Taiwan and the tectonic significance. Acta Seism. Sin. (to appear). (in Chinese)

Yamashita, T., 1998: Simulation of seismicity due to fluid migration in a fault zone. *Geophys. J. Int.*, **132**, 674-686, doi: 10.1046/j.1365-246X.1998.00483.x. [Link]

Yamashita, T. and L. Knopoff, 1987: Models of aftershock occurrence. *Geophys. J. R. astr. Soc.*, **91**, 13-26, doi: 10.1111/j.1365-246X.1987.tb05210.x. [Link]

Yen, T. P., 1985: A review of the filed survey of the 1935 Hsingchu-Taichung earthquake. Proc. Seminar Commem. 50th Ann. for Hsinchu-Taichung Earthquake of 1935, 11-17. (in Chinese)

Yu, S. B., Y. S. Cheng, and Y. B. Tsai, 1977: Aftershocks of the Wufeng, Chiayi earthquake of April 14, 1976. *Acta Geol. Taiwanica*, **19**, 62-73.

Ziv, A. and A. M. Rubin, 2003: Implications of rate-and-state friction for properties of aftershock sequence: Quasi-static inherently discrete simulations. *J. Geophys. Res.*, **108**, B1, 2051, doi: 10.1029/2001JB001219. [Link]